Spring 2023

MESOSCALE EXPERIMENTAL PROTOCOL FOR OIL MOVEMENT UNDER SEA ICE

Jessica Manning
University of New Hampshire, Durham

Follow this and additional works at: https://scholars.unh.edu/thesis

MESOSCALE EXPERIMENTAL PROTOCOL FOR OIL MOVEMENT UNDER SEA ICE

BY

JESSICA R. MANNING

Bachelor of Science, Environmental Engineering, University of New Hampshire, 2021

THESIS

Submitted to the University of New Hampshire

in Partial Fulfillment of

the Requirements for the Degree of

Master of Science

in

Civil and Environmental Engineering

May, 2023

This thesis has been examined and approved in partial fulfillment of the requirements for the degree of Master of Science in Civil and Environmental Engineering by:

Nancy E. Kinner
Thesis Director
Professor of Civil and Environmental Engineering

Thomas P. Ballestero
Professor of Civil and Environmental Engineering

Diane L. Foster
Professor of Mechanical Engineering and Ocean Engineering

on January 31, 2023

Original approval signatures are on file with the University of New Hampshire Graduate School.

Acknowledgements

I would like to thank my advisor, Dr. Nancy Kinner, for all the guidance over the years. This project would not have succeeded without her support, knowledge, and persistence. I would also like to thank Kathy Mandsager for all the help and coordinating efforts. I am beyond thankful to have joined the Coastal Response Research Center and am grateful for the funding and unique experiences we have had along the way.

I would like to thank my Advisory Committee for dedicating their time and efforts to provide advice for this project. Their expertise has elevated the outcome of this project. This committee includes Chris Barker, Kelsey Frazier, Debbie French-McCay, Melissa (Missy) Gloekler, Amy MacFadyen, Ted Maksym, Marc Oggier, Scott Socolofsky, and Jeremy Wilkinson. Special thanks to Missy Gloekler for constructing the MacFarlane Flume used in this project and always making time to answer questions and help troubleshoot any issues I encountered. And thank you to Ora and the late Neil MacFarlane for providing funding for the flume's construction.

Thank you to John Ahern and Scott Campbell for assisting with technical design and construction, and for teaching me in the process. Thank you to Tom Ballestero and Diane Foster for sitting on my Thesis Committee and providing thoughtful recommendations for this project.

Finally, I would like to thank my peers who have worked diligently along my side. This includes Elsa Goldsberry, Alice House, Kaylee Molan, Rowan Pow, Christian Ruiz Robles, Melianys Ruperto-Gonzalez, and Will Stark. In particular, I'd like to acknowledge Tori Sweet, Kara Wittmann, and James Wood for the extended number of hours and memorable moments they have spent in the lab. And a special thank you to Chris Keohane and his father for going out of their way to help set up chillers to reach our goal water temperature.

Table of Contents

List of Figures

List of Tables

List of Abbreviations

ADAC: Arctic Domain Awareness Center

ADIOS: Automated Data Inquiry for Oil Spills

ADV: Acoustic Doppler Velocimeter

AMSM: Oil Spill Modeling for Improved Response to Arctic Maritime Spills: The Path Forward

BSEE: Bureau of Safety and Environmental Enforcement

CRRC: Coastal Response Research Center

CSS: Critical Shear Stress

FOSC: Federal On-Scene Coordinator

GNOME: General NOAA Operational Modeling Environment

HOOPS: Hoover Offshore Oil Pipeline System

ICS: Incident Command System

NCP: National Oil and Hazardous Substances Pollution Contingency Plan

NIC: National Ice Center

NOAA: National Oceanic and Atmospheric Administration

NOAA OR&R: NOAA Office of Response and Restoration

OPA: Oil Pollution Act of 1990

OSLTF: Oil Spill Liability Trust Fund

SOP: Standard Operating Procedure

SOTT: Sunken Oil Transport Tool

SSC: Scientific Support Coordinator

UNH: University of New Hampshire

USCG: United States Coast Guard

Abstract

Decreasing sea ice extent in the Arctic provides more opportunities for human activities (e.g., shipping, development) and increases the likelihood of Arctic oil spills. Sea ice adds complexity into oil spill models because it has significant impacts on oil fate and behavior. Understanding these complexities will improve Arctic oil spill responses and mitigate impacts. As part of a recent project on Arctic response conducted by the Coastal Response Research Center (CRRC), sea ice and oil spill modelers concluded that further research is needed to model the behavior of oil under ice. The underside of sea ice is affected by waves, currents, winds, and snow cover over time and form shapes of various sizes. Experiments designed and conducted in the MacFarlane Flume at the University of New Hampshire (UNH) are used to better understand the movement of oil under sea ice. Blocks of ice are formed in customized welded boxes (36" length x 11.75" width x 10" depth). An ellipse half cylinder cavity is shaped into the underside of one of the blocks to simulate a typical under ice conformation. The shape and size were recommended by sea ice and oil spill modeling experts on the project's advisory committee. The ice blocks are secured in the flume and a known volume of oil is injected into the cavity. Water relative velocity is controlled at fine increments (~0.1 m/s; ~0.2 kts) to analyze the movement of oil with respect to the fuel type and temperature. The oil used for preliminary experiments was Hoover Offshore Oil Pipeline System (HOOPS) oil, and oil transport from the cavity was observed at 0.16 +/- 0.03 m/s (0.31 +/- 0.06 kts). Data collection using the equipment and developed methods during this thesis research will enhance the CRRC's ability to determine the coefficients needed for spill models to predict oil movement under sea ice.

1. Motivation and Background

The Arctic environment plays a vital role in the global climate system (Perovich et al., 2020). It regulates climate temperature and is a habitat for many marine mammals, birds, fish, and about four million people (Thompson, 2016). A healthy Arctic ecosystem is essential for people who rely on subsistence-based activities to survive and preserve their culture. Figure 1 displays indigenous and non-indigenous populations in the Arctic by country.
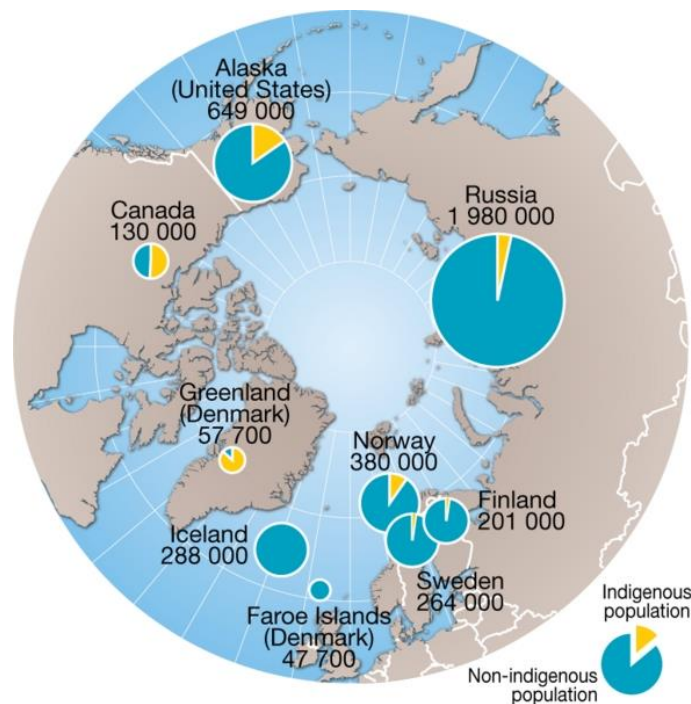
Figure 1: Map of Arctic populations (Ahlenius, 2008).

Despite its importance, the Arctic is at risk for larger and/or more frequent oil spills (Wilkinson et al., 2017). Because the Arctic experiences climate change at higher rates than anywhere else on the planet, sea ice has decreased in extent by 12% per decade since 1981 (NASA, 2022) (Figure 2).
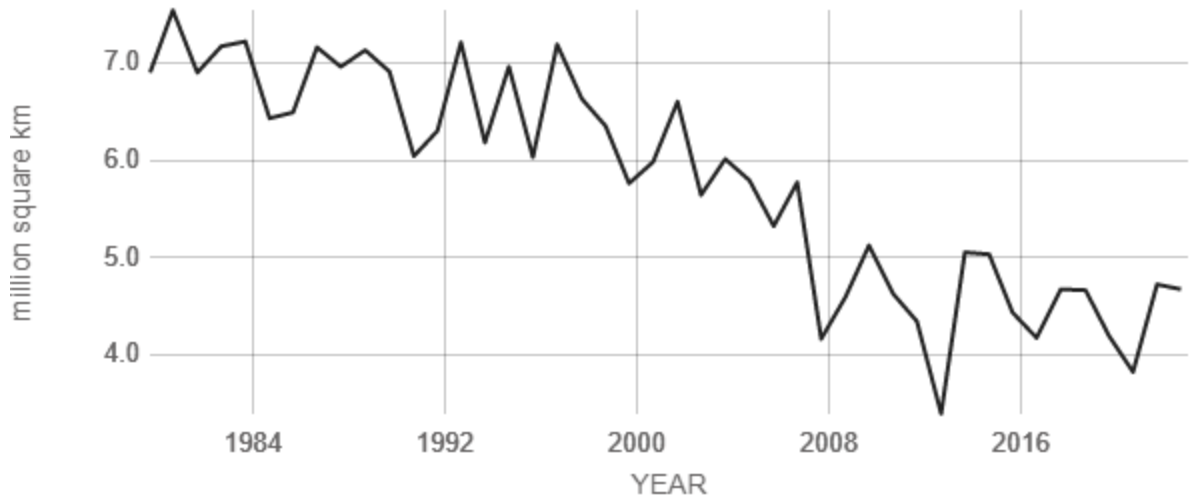
Figure 2: Decrease in sea ice extent (NASA, 2022).

Furthermore, sea ice has a much larger albedo than the open ocean, reflecting up to 85% of incident shortwave radiation, while the ocean reflects less than 10% (Persson & Vihma, 2017). Open water absorbs and retains more heat, which exacerbates climate change, and then melts more sea ice, accelerating the cycle. This creates a positive feedback loop (Notz & Bitz, 2017) (Figure 3). Other positive feedback loop examples include the thaw of permafrost and coastal erosion, that release greenhouse gases to further accelerate the rate of climate change (Nielsen et al., 2022).
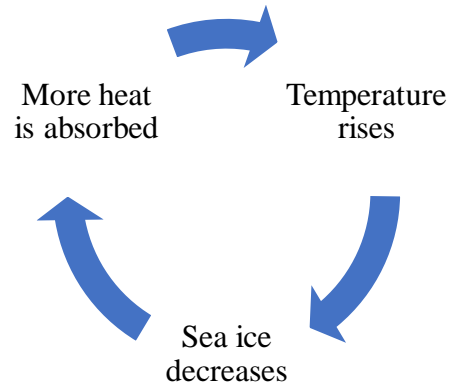
Figure 3: Sea ice melt positive feedback loop.

There has also been a decrease in multiyear ice, as well as shortened growing seasons (Comiso, 2012; Markus et al., 2009). Multiyear sea ice, that persists through the summer for more than one season, has retreated to the central Arctic Ocean (Comiso, 2012). The shortened growing seasons suggest that ice will begin to freeze later and start to melt sooner (Markus et al., 2009). Decreased sea ice opens shipping routes (e.g., Northwest Passage, Northern Sea Route) (Figure 4) and this increased accessibility leads to more development (Rodrigue, 2020).
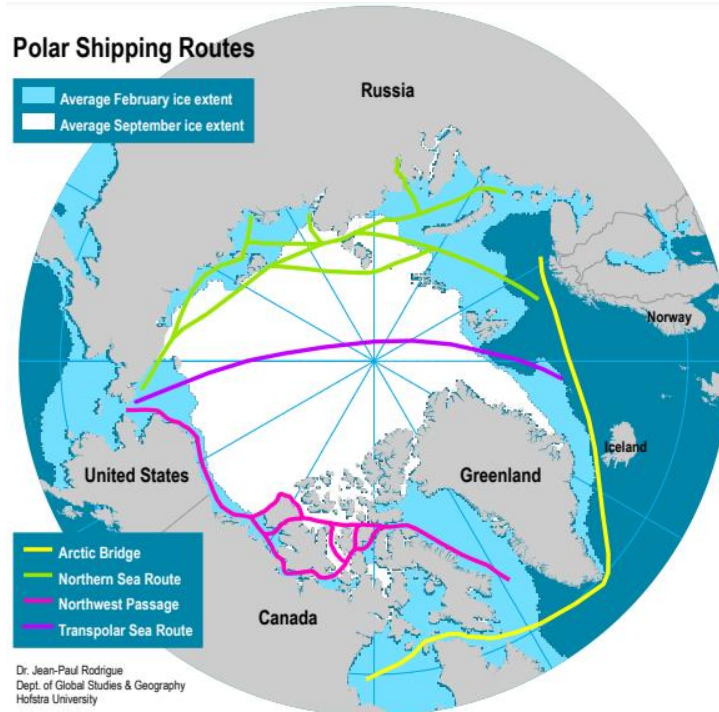
Figure 4: Arctic Sea Routes (Rodrigue, 2020).

Increased access to Arctic shipping routes has spurred vessel traffic in those areas, as they provide more direct routes from Asia to Europe and vice versa and save resources and time. Therefore, the likelihood of shipping accidents involving oil spills in the Arctic is increasing (Forsman, N. & Forsman, B., 2019). There are more operational challenges in the Arctic than other regions that can hinder oil spill response efforts (e.g., large distance for equipment and personnel to travel, 24 hours of darkness in the winter months, severe weather conditions). Therefore, oil spill model predictions are crucial for successful response (Manning et al., 2021).

Spill response decision-making is guided by model outputs that predict oil fate and transport. In the United States (U.S.), the National Oceanic and Atmospheric Administration (NOAA) uses the General NOAA Operational Modeling Environment (GNOME) to predict oil movement in the environment (Zelenke et al., 2012). A NOAA scientific support coordinator

(SSC) works closely with a U.S. Coast Guard (USCG) federal on-scene coordinator (FOSC). This structure is defined by the National Oil and Hazardous Substances Pollution Contingency Plan (NCP) which states that the Incident Command System (ICS) is used to facilitate response. The NCP was revised in accordance with the Oil Pollution Act (OPA) of 1990. OPA also established the Oil Spill Liability Trust Fund (OSLTF) by taxing domestic crude oil and imported petroleum products by the barrel. This provides immediate funding for response actions in an emergency even if a responsible party is not identified (National Pollution Funds Center, 2006).

Oil spill model uncertainty poses further challenges for response decision-making and is heightened in Arctic conditions because sea ice is a complicating factor that influences oil fate and transport. In addition to model uncertainties, visual observations are also challenged by Arctic conditions; oil is not easily detectable under or near sea ice. These additional uncertainties reduce the effectiveness of response and cleanup efforts, which can lead to devastating impacts to Arctic ecosystems and communities (Manning et al., 2021).

Thus, it is crucial to better understand and model the interactions between sea ice and oil. GNOME currently contains a simplified sea ice algorithm, called the 80/20 rule. The 80/20 rule suggests that oil moves as it would in open water when the sea ice concentration is less than 20%, it moves with the ice when the concentration is greater than 80%, and drifts proportionally to the ice when the concentration is between 20% and 80% (Figure 5). As sea ice concentration reaches 80%, oil particle velocity is equivalent to that of the sea ice (Zelenke et al., 2012).
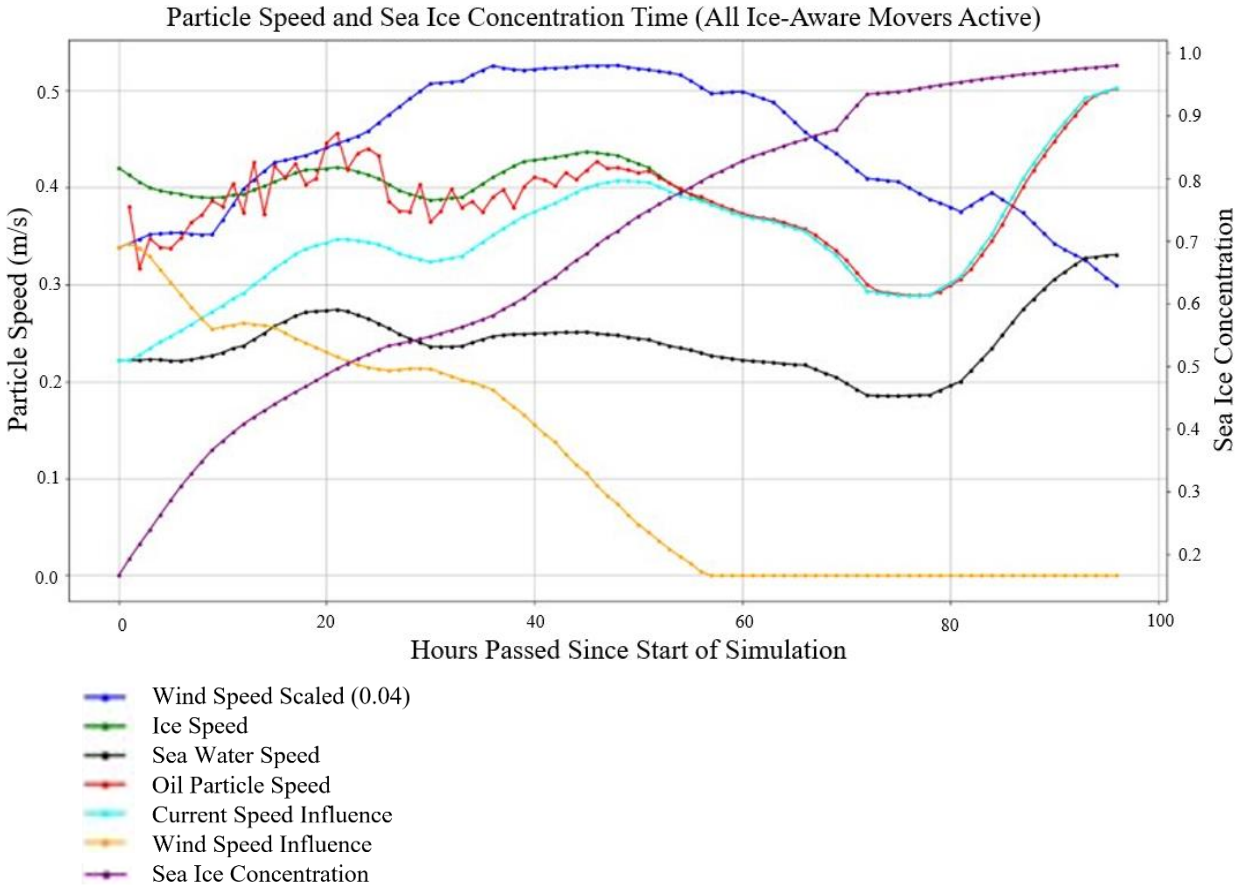
Figure 5: Example GNOME output.

Sea ice concentration and velocity (direction and speed) must be collected from numerical sea ice models, and input into GNOME along with hydrodynamics and data from NOAA's Automated Data Inquiry for Oil Spills (ADIOS). ADIOS calculates oil weathering (e.g., evaporation, dispersion) based on oil properties (e.g., pour point, density, viscosity) and environmental conditions (e.g., wind speed and direction, water temperature, current speed and direction). GNOME uses this data and the 80/20 rule to estimate the oil's trajectory. When there is less than 20% sea ice concentration, weathering will occur as it would in open water; when there is greater than 80% sea ice concentration, weathering will not occur, and when there is between 20% and 80% sea ice concentration, weathering is proportionally reduced from its rate

in open water (Zelenke et al., 2012). This results from the presence of sea ice, and cold temperatures reduce oil spreading, evaporation, as well as dispersion and emulsification caused by wave action in open water (Wilkinson et al., 2017).

Recent work has been conducted to improve GNOME's Arctic capabilities. The Arctic Domain Awareness Center (ADAC) Oil Spill Modeling for Improved Response to Arctic Maritime Spills: The Path Forward (AMSM) project examined the state-of-the-art oil spill models, sea ice models, and sea ice forecasting systems. (N.B., Sea ice forecasting systems incorporate sea ice knowledge with sea ice models to produce a final product.) ADAC AMSM worked with modelers and forecasters to understand sea ice outputs that could be used as oil spill model inputs to improve trajectories. The modelers defined their file formats and the most important sea ice characteristics, as oil and sea ice interact in several different ways. Figure 6 demonstrates these interactions, as well as other potential oil interactions in the Arctic environment. For example, oil can become encapsulated in the sea ice if it is spilled during the growth season (typically September – March) (Oggier et al, 2020). Oil can also migrate upwards through the sea ice via leads (vertical fractures) or during the spring and early summer when permeability increases (Oggier et al, 2020).
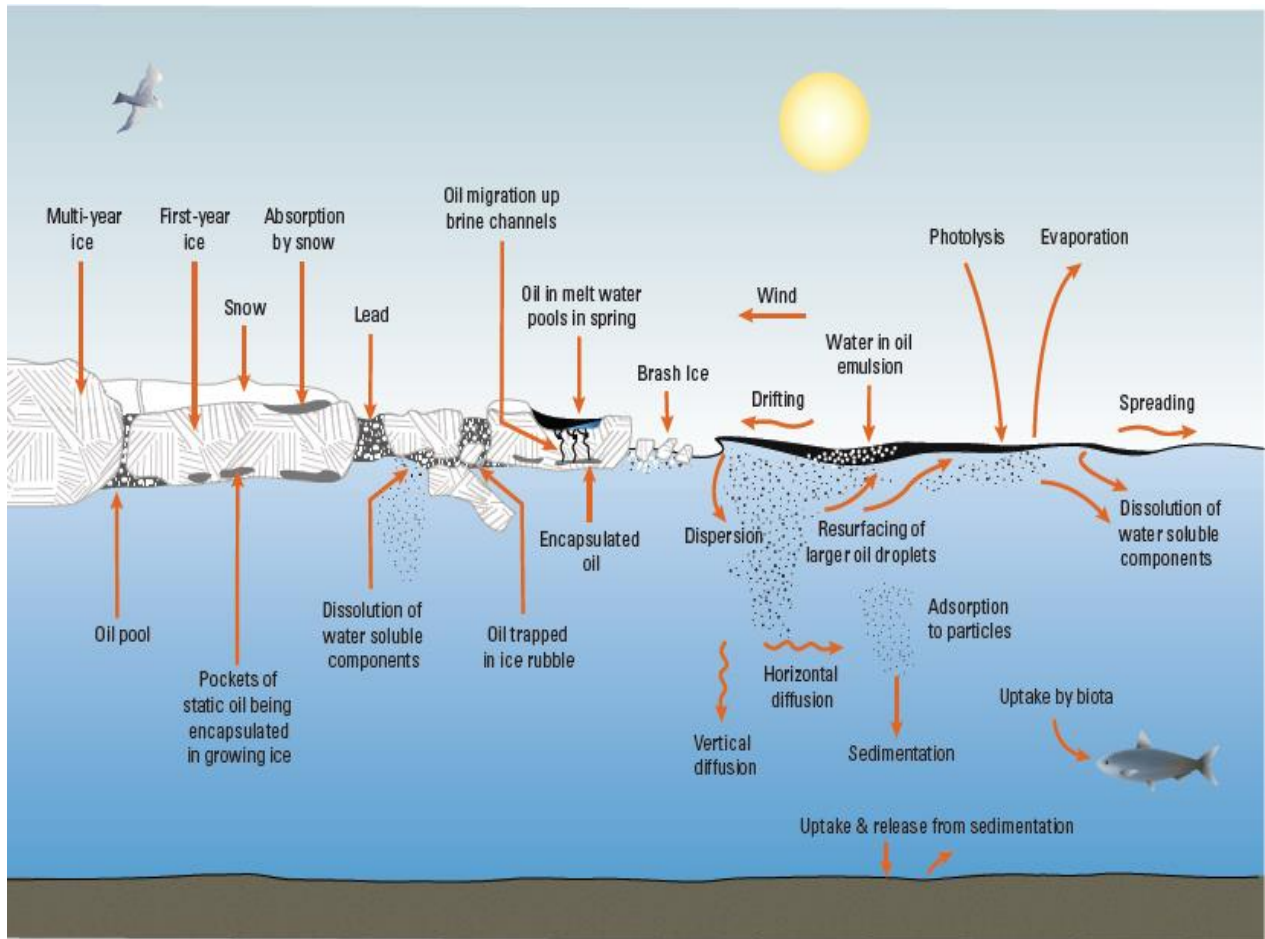
Figure 6: Oil and ice interactions (Daling et al., 1990).

Discussions about these interactions during the AMSM project led to the conclusion that a major interaction is oil movement under sea ice. This is supported by a study conducted in Prudhoe Bay, where oil was released under sea ice and its spreading was limited as it filled and was contained by undulations under the sea ice (Glaeser et al., 1971). The underside of sea ice is shaped by winds, waves, currents, and differences in snow cover that form protrusions of different sizes. The sizes are related to sea ice age and surface conditions.

Sea ice draft (distance of sea ice below water level) has been measured with different techniques (e.g., radio echo sounding, acoustic sounding, drilling holes through ice, photographs

from divers). Kovacs et al. (1981) studied three sites off the coast of Prudhoe Bay, AK in March 1980 using a radio echo sounding system under each leg of an equilateral triangle laid over each site. Under ice topography results from a site of undeformed first year sea ice with even snow cover are graphed by ice thickness over the distance of each leg (Figure 7). Ice thickness is the sum of sea ice draft and freeboard (ice thickness above water surface).
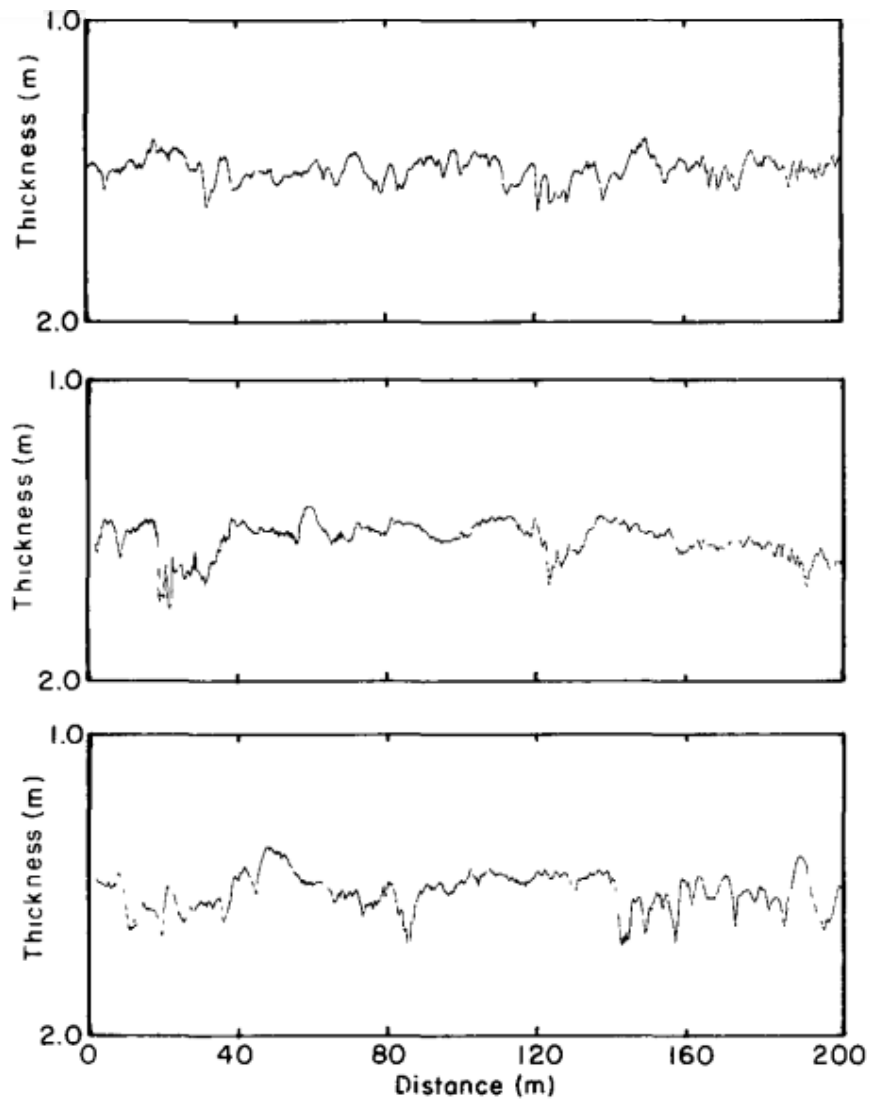
Figure 7: Under ice topography off the coast of Prudhoe Bay (March 1980) (Kovacs et al., 1981).

Oil can enter protrusions under sea ice by several routes. For example, encapsulated oil can be released during the melt season (typically March – September) in the Arctic and then become trapped under ice. Oil in open water can travel with currents and encounter an ice floe and be pushed underneath it. Oil released under sea ice (e.g., from a subsurface pipeline rupture, vessel collision, grounding) can rise through the water column until it reaches the ice interface. Winds and currents can move ice floes together, squeezing the oil and allowing it to pool. Conversely, as ice floes move apart, oil can spread over a larger area.

Frazier (2019) used ice "egg codes," provided daily by the U.S. National Ice Center (NIC) to better understand under ice roughness based on in situ conditions. These codes present the total concentration of ice cover, partial concentrations of the three thickest ice types, stages of development including age and thickness for the same three thickest ice types, and form of the sea ice or ice floe size for the three thickest ice types (Figure 8).
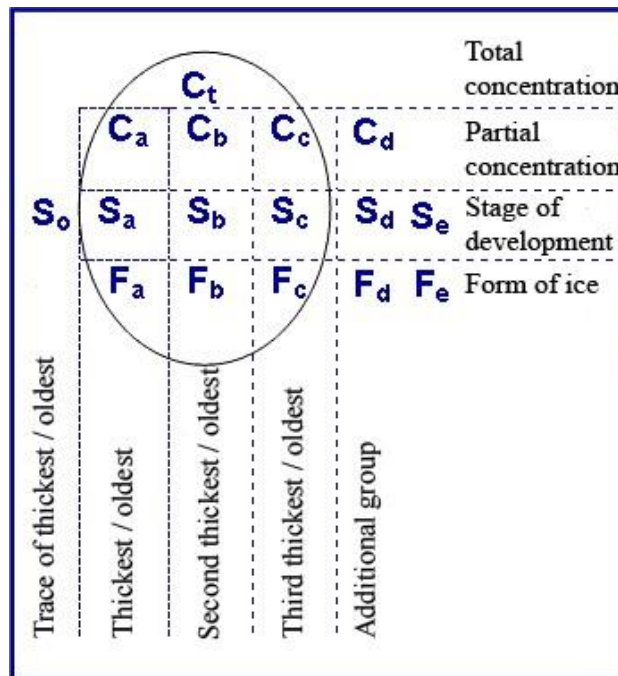
Figure 8: Ice Egg Code (ECCC, 2016).

Table 1 describes the coding used for the sea ice stages. Each ice egg code provides three numbers separated by commas for stages of the three thickest types of ice within the given region. Original ice egg codes use single digit numbers and asterisks, which Frazier's modified code converted to all digits for ease of graphing and visualization. The lower modified codes correspond to newer, thinner ice, while the higher values correspond to older, thicker ice. (N.B., Frazil ice is the formation of ice crystals at the start of the freezing process. Nilas are thin sheet formation on the water's surface. Ice rind is brittle, shiny formation of a very thin ice sheet. Fast ice is immobile and anchored to either the shore, ocean bottom, or grounded ice bergs.)

Table 1: Ice stage code (Frazier, 2019).

Ice Egg Code	Frazier's Modified Code	Thickness (cm)	Description
1	1	0-10	New, Frazil, Slush, etc.
2	2	10-30	Nilas, Ice Rind
3	3	10-15	Young
4	4	15-30	Gray
5	5	15-30	Gray - White
6	6	30-200	1Y[1]
7	7	30-70	1Y, Thin
8	8	30-70	1Y, Thin, Stage 1[2]
9	9	30-70	1Y, Thin, Stage 2[3]
1*	10	70-120	1Y, Medium
4*	11	>120	1Y, Thick
7*	12	>200	Old 1Y Ice
8*	13	>200	SY[4]
9*	14	>200	MY[5]

[1]1Y = first year
[2]Stage 1 = 30-50 cm thick
[3]Stage 2 = 50-70 cm thick
[4]SY = second year
[5]MY = multiyear

Frazier compared these data to under ice storage capacity estimates, which she calculated using upward looking sonar data collected over five years from two locations in the U.S. Arctic (Beaufort and Chukchi Seas). Upward looking sonar measured the ice draft which she used to calculate under ice storage capacity. Another method to determine ice draft is to subtract the ice freeboard from the total ice thickness, if these are known values (Wilkinson et al., 2007). Under ice storage capacity was calculated using an equation developed by LeSchack and Chang (1977) (Equation 1).

$$\delta_{sc} = \frac{\iint \left((h'_{ice} > h_{mean}) - h_{mean} \right) dx\, dy}{A_d} \qquad (1)$$

Where,

δ_{sc} = storage capacity of the ice (m^3/km^2 ice),

h'$_{ice}$ = ice draft at a position at (x, y) (m),

h$_{mean}$ = mean ice draft over a given length (m),

and A$_d$ = domain area of ice surface (km^2).

This equation defines potential volume of oil pooling under ice as a function of the volume above the mean sea ice draft, but the equation needs to be validated with experimental data. Figure 9 shows the general trend of under ice roughness increasing with sea ice stage (Frazier, 2019).
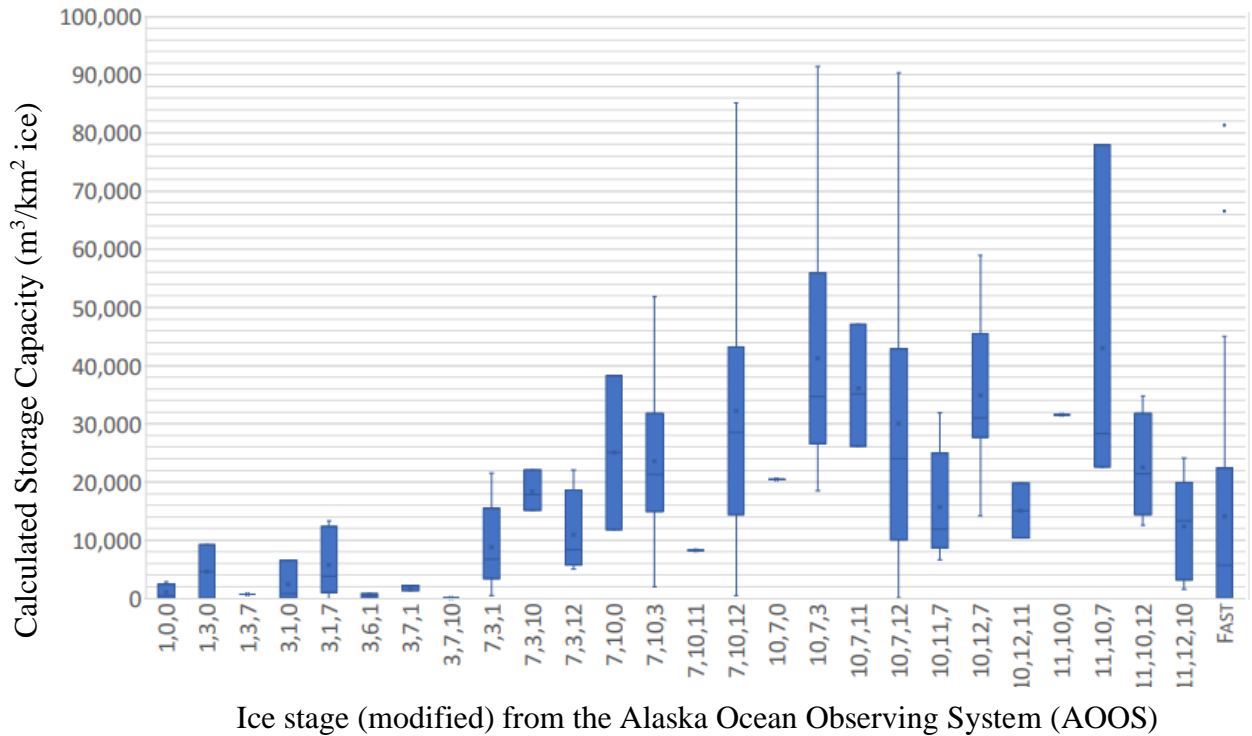
Figure 9: Ice stage (modified code) (Table 1) vs. calculated storage capacity (m^3/km^2) (Frazier, 2019).

Under ice storage capacity has the potential to trap large volumes of oil and prevent it from moving with the currents (Glaeser et al., 1971). There is limited research available investigating the storage capacity relationship, which oil spill response models could use to improve their trajectories. Experiments are needed to collect data that will help determine the movement of oil under sea ice as a function of under ice roughness and currents.

2. Goals / Objectives of the Thesis Research

Oil spill response models (e.g., GNOME) use the 80/20 rule as a simplified algorithm to predict oil movement in ice covered areas. Under ice roughness and storage capacity are not considered in model predictions. Increased activity and interest in the Arctic require improvements for oil spill models, particularly with regards to the movement of oil under ice. Oil spreading under ice has not been well studied and contributes to model trajectory uncertainties.

Experimental or observational data is required to update oil spill models. In the U.S., intentional releases of oil in the environment are prohibited by environmental regulations (i.e., Clean Water Act), and studies conducted in the Arctic face technical challenges (e.g., limited resources, transportation difficulties). Thus, oil-related experiments under Arctic conditions must be designed and executed in a laboratory setting. This setting must replicate actual environmental conditions as much as possible, while having set controls and the ability to collect data efficiently. The design must be tested and adjusted to achieve an optimized protocol. The overall goal for this project was to design and execute standard protocols to better understand the movement of oil under ice, using a specific under ice cavity. This project was divided into the following three phases:

1. Replicate Arctic conditions.
2. Freeze ice blocks with a specified under ice cavity and secure in flume.
3. Develop a repeatable experimental protocol to monitor the behavior of oil under ice.
   a. Inject known volume of oil.
   b. Measure relative velocity of water under ice.
   c. Record oil movement within and outside the cavity.

3. Materials

The following are required equipment and their purposes to successfully run experiments. Design processes are explained in Section 4: Methods.

- Insulated recirculating flume: Replicate ocean currents under sea ice. The MacFarlane Flume (Figure 10) at the University of New Hampshire (UNH) is a 600-gallon recirculating flume with a top and bottom section. Water movement is driven by two 10 hp motors, each with a 10 3/8-inch propeller. Water velocity is relative to ice velocity which is assumed zero in all directions. Two variable frequency drives control each motor at 0.1 Hz intervals, which can manipulate under ice relative velocity at 0.08 +/- 0.02 m/s intervals from 0.06 +/- 0.01 m/s (1 Hz) to 1.04 +/- 0.05 m/s (14 Hz) under uniform and steady state conditions. The top flume section is 13 ft long, 1 ft wide, and 1 ft 10 inch deep. The bottom section is 16 ft long, 4 ft wide, and 1 ft deep. The flume is insulated using RMax Thermasheath polyisocyanurate rigid foam insulation board (Figure 11). The rigid, foil-faced insulation makes tight connections which are sealed with foil tape. Ports are cut into the insulation for access and viewing (Figure 11a).
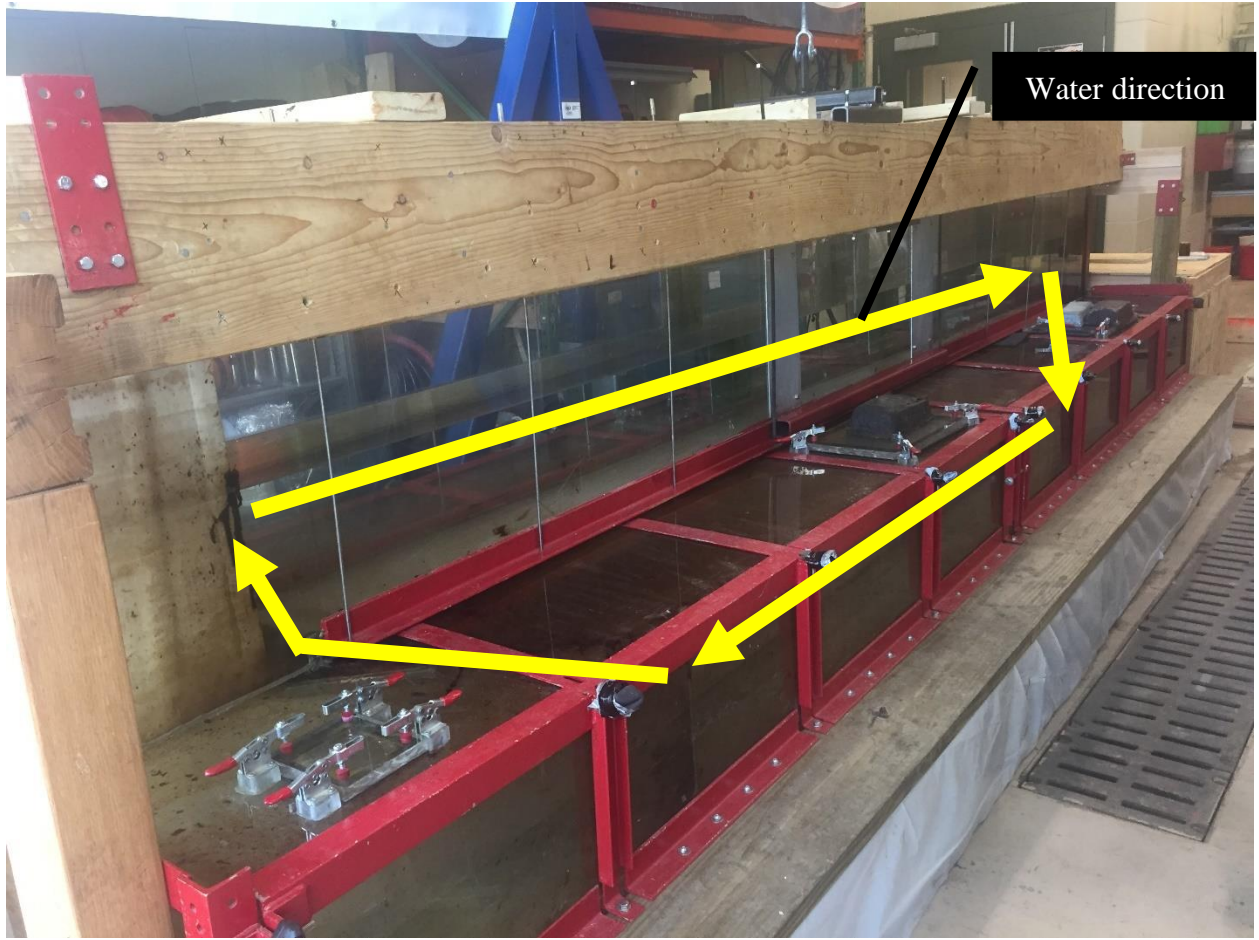
Figure 10: MacFarlane Flume without insulation.
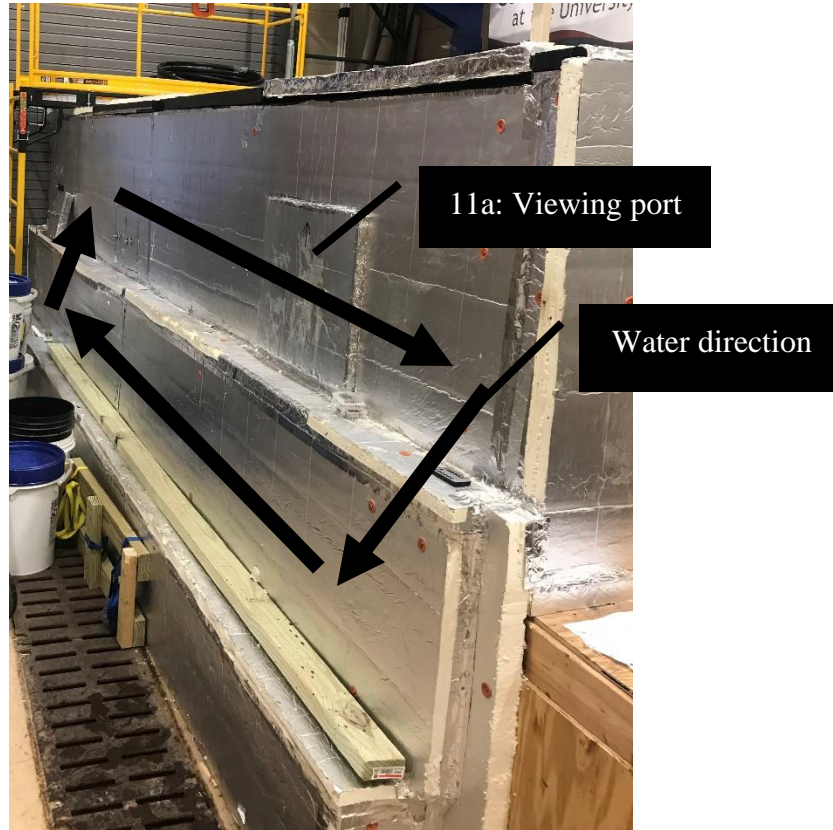
Figure 11: MacFarlane Flume insulated.

- Air conditioner: Cool air between flume and insulation.

- Chillers: Chill water in flume (Figure 12). A Goulds Water Technology 0.5 hp centrifugal pump (1BF50512; Bluffton, IN) (Figure 13a) is used to circulate the flume water through two heat exchangers (Figure 13b) which are connected to two closed loop Neslab HX-150 recirculating chillers (Waldwick, NJ) (Figure 13c), and then through two open loop Copeland Quality chillers (RRG4-0100-PAA-202; Sidney, OH) (Figure 13d). Skirtboard rubber (1/2" thickness; Grainger; BULK-RS-SBRHS60-69; tensile strength: 1,000 psi) is placed under the Copeland Quality chillers to absorb vibrations. The heat exchangers are Bell & Gossett (350,000 BTU/hr Low Pressure BPX Brazed Plate Heat Exchanger; BP411-10LP; Buffalo, NY) and GEA Heat Exchangers, Inc. PHE Division (225,000 BTU/hr; FG5X12-24; York, PA). Plumbing consists of 1" PVC (schedule 40) pipe and adapters and vacuum-rated PVC tubing (Kuriyama of America Inc.; Schaumburg, IL; 9118T3; 1" ID, 1-7/16" OD, internally reinforced with yarn and steel wire, rated for a maximum pressure of 220 psi at 72°F). Eight union fittings are placed in the setup to provide points of access for potential troubleshooting and reconfiguration (Figure 12). The tubing connected to the Neslab HX-150 chillers is flexible to accommodate any movement (Figure 12).
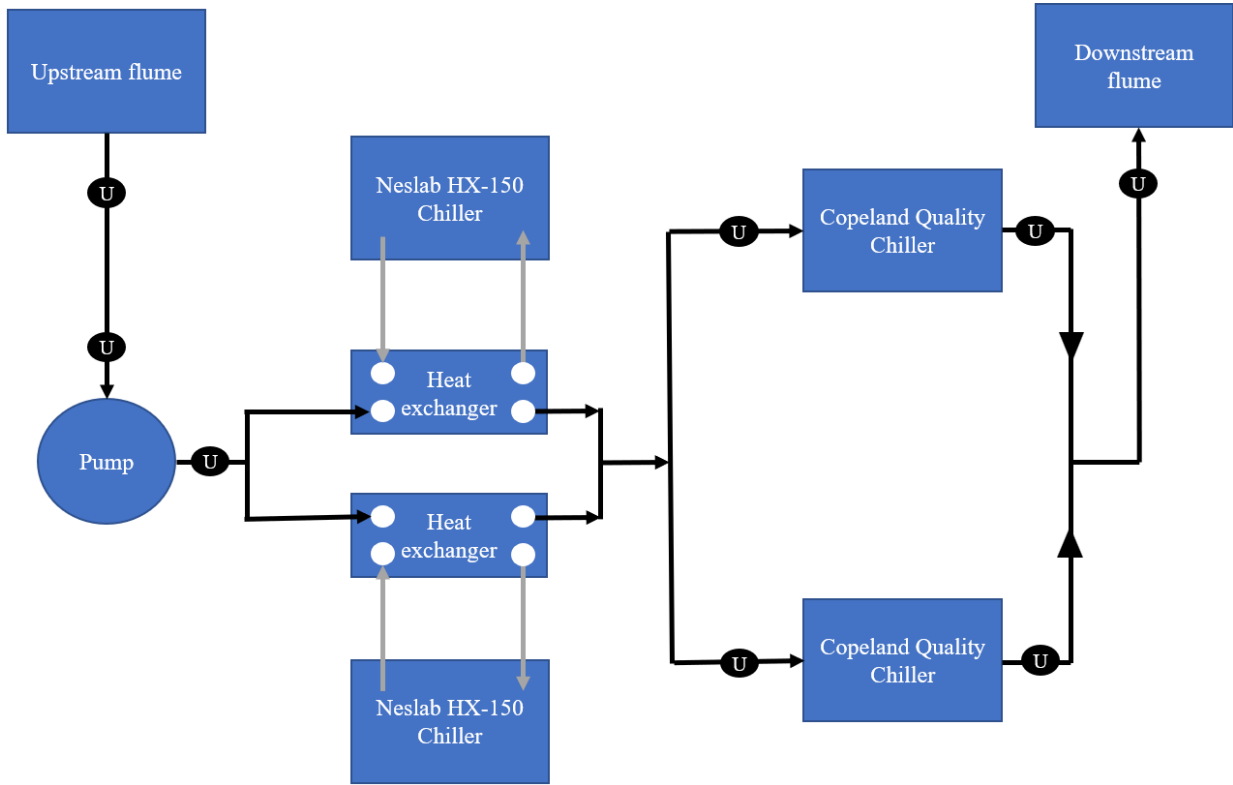
Figure 12: Water chiller configuration. Black lines = PVC pipes; gray lines = tubing; U = union fitting.
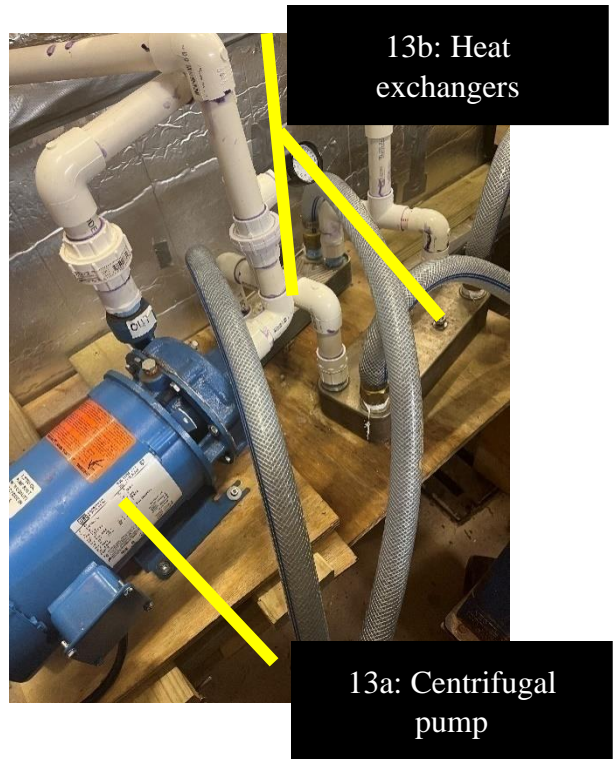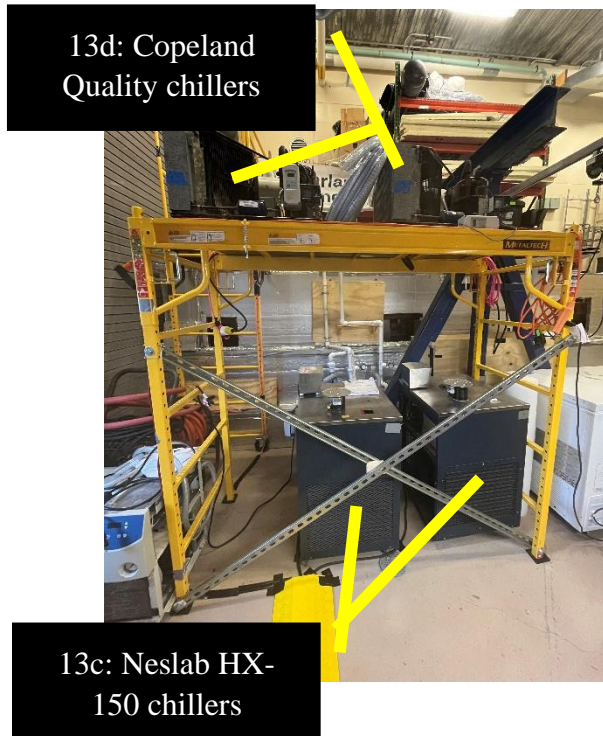
Figure 13: Images of centrifugal pump, heat exchangers, and chillers.

- Chest freezers on wheels: Two 24.8 ft^3 Frigidaire chest freezers (FFFC25M4TW and FFCL2542AW) are used to create ice blocks and transport them under a hoist. Each freezer has a shelf so it can store five ice blocks.

- Welded ¼" 5052 aluminum boxes (Custom Sheet Metal; Manchester, NH): Shape ice

    blocks in customized boxes which each have interior dimensions 36" length x 11.75"

    width x 10" depth (Figure 14). One box contains a mold in the center of the box's

    lengthwise span to form an ellipse half cylinder (9" length x 11.25" width x 3" depth)

    cavity in the underside of the ice (Figure 14a). This shape was recommended by the

    advisory committee based on probable environmental conditions. The other box forms a

    block with a flat bottom (Figure 14b) to stabilize the flow under ice upstream of the ice

    cavity. The ice block with the cavity weighs about 132 lb., while the ice block with the

    flat bottom weighs about 140 lb. C-shaped wooden supports are placed across the top of

    each welded box while ice is freezing to prevent the sides and welds from bowing

    outward (Figure 15).

Figure 14a: Ice box with cavity

Figure 14b: Ice box with flat bottom

Figure 14: Welded ice boxes.
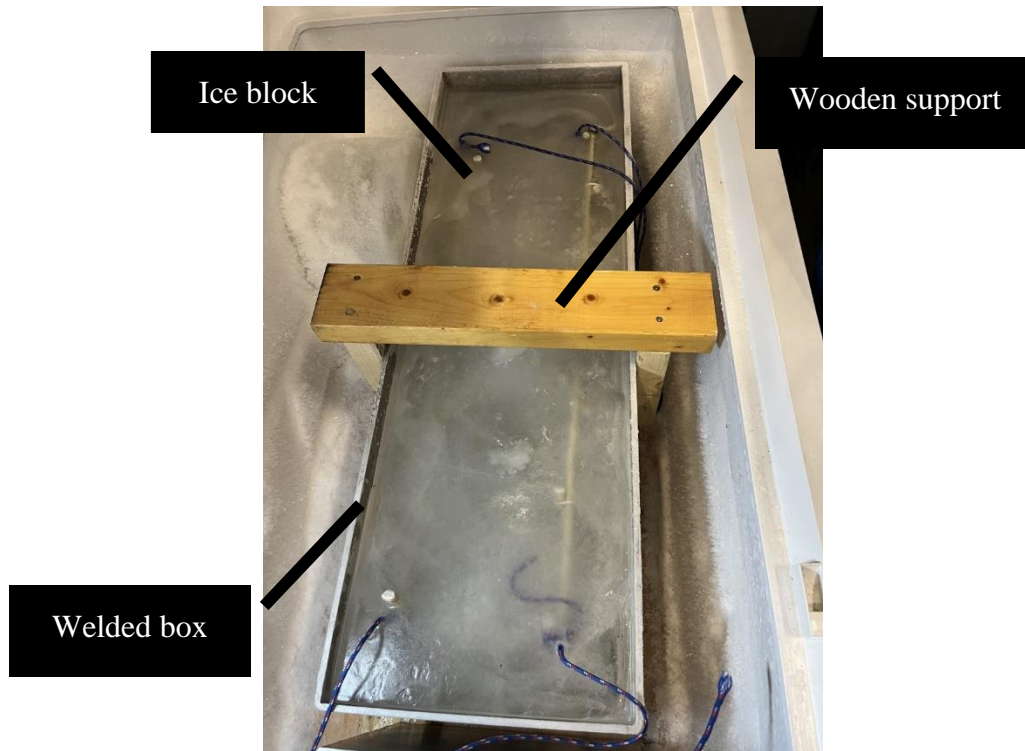
Figure 15: Wooden support for welded boxes.

- Fiberglass rebar structure with hook: Maintain ice block integrity while it is lifted into the flume by a hook frozen in the ice (Figure 16a). The fiberglass rebar structure (1/2" diameter; tensile strength = 690 MPa) runs along the perimeter of the top of the ice block and has cross beams for support (Figure 16). It also has rebar that runs down the depth along each side of the ice block. The segments are connected with twisted wire (Figure 16b). The hook is attached to the center of the rebar cross beams.
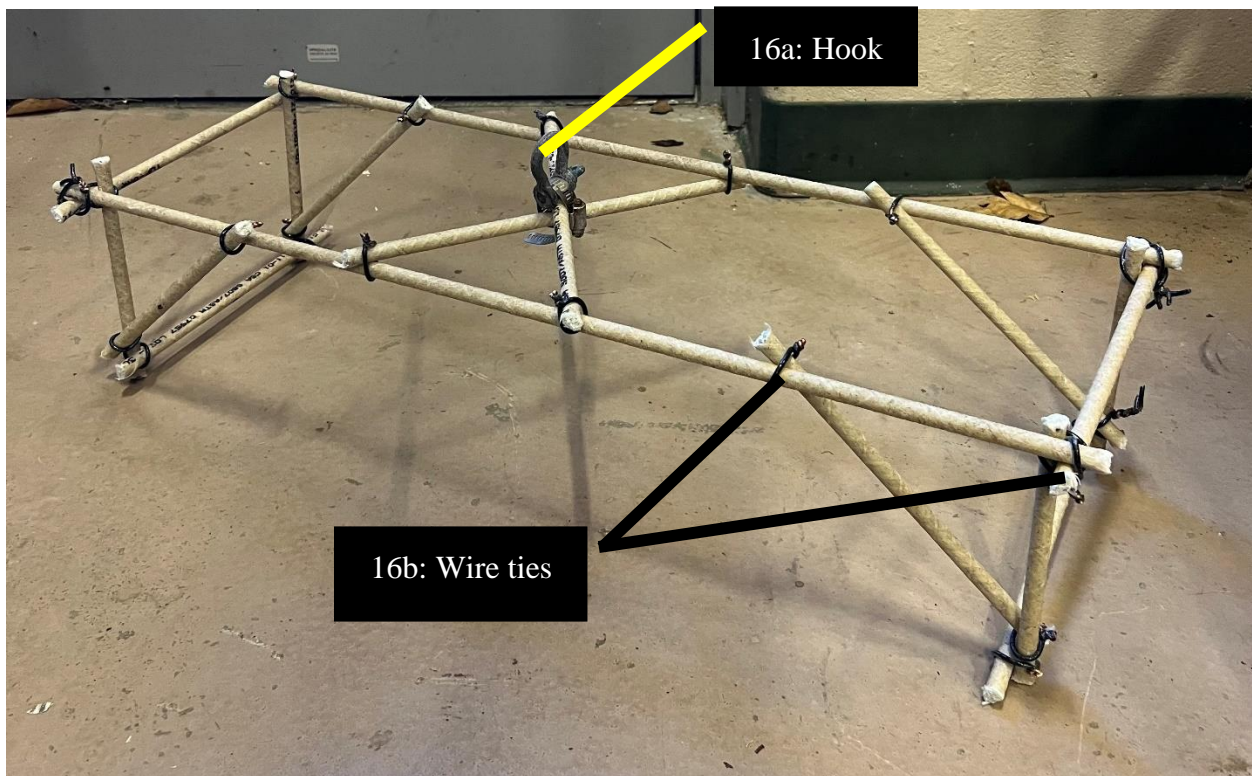
Figure 16: Fiberglass rebar structure with hook.

- Polycarbonate sheets and rods: Prevent oil from traveling across the width of the flume within the ice cavity and leaking out the sides of the ice block, which was slightly narrower than the flume walls (Figure 17). The sheets (Grainger BULK-PS-PC-101; thickness: 1/4"; tensile strength: 9,700 psi) (Figure 17a) are placed along the ice cavity and are held in place with perpendicular polycarbonate rods (Grainger 2XPX2; diameter: 1/2"; tensile strength: 10,500 psi) (Figure 17b). A radius is carved into the bottom of the polycarbonate sheet (Figure 17c) to fit tightly in the welded box (Figure 18). There are additional acrylic pieces, "wings," that protrude into the ice block to prevent oil from leaking out along the polycarbonate edge (Figure 17d).
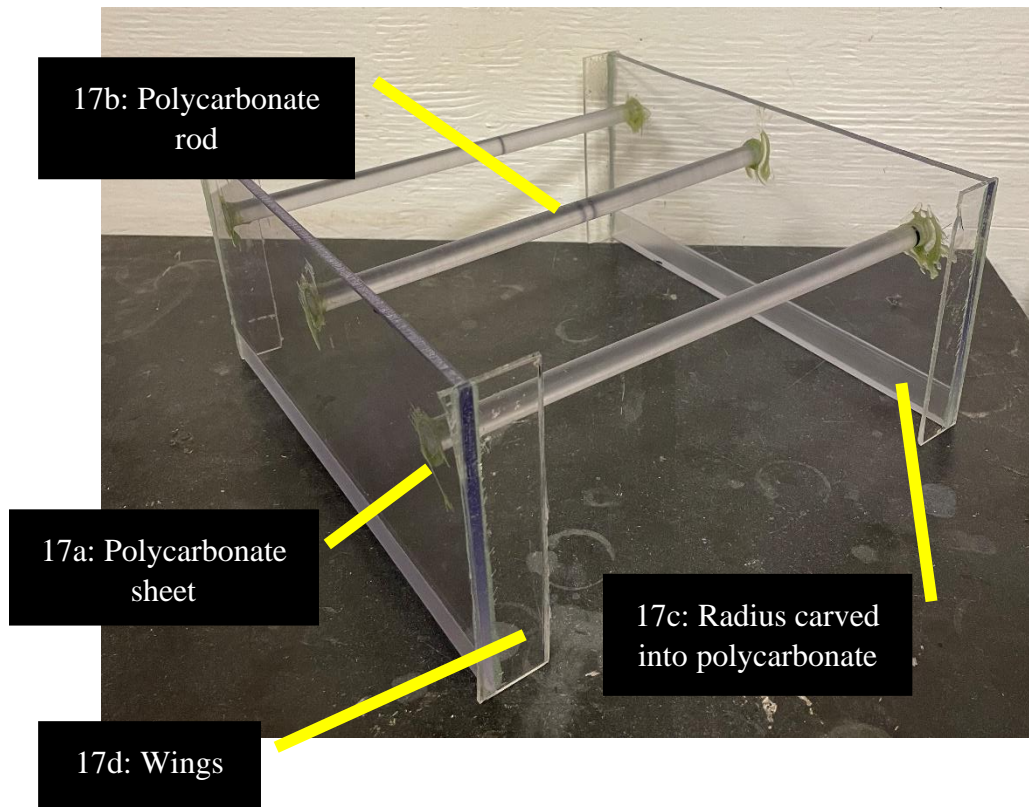
Figure 17: Polycarbonate sheets and rods.
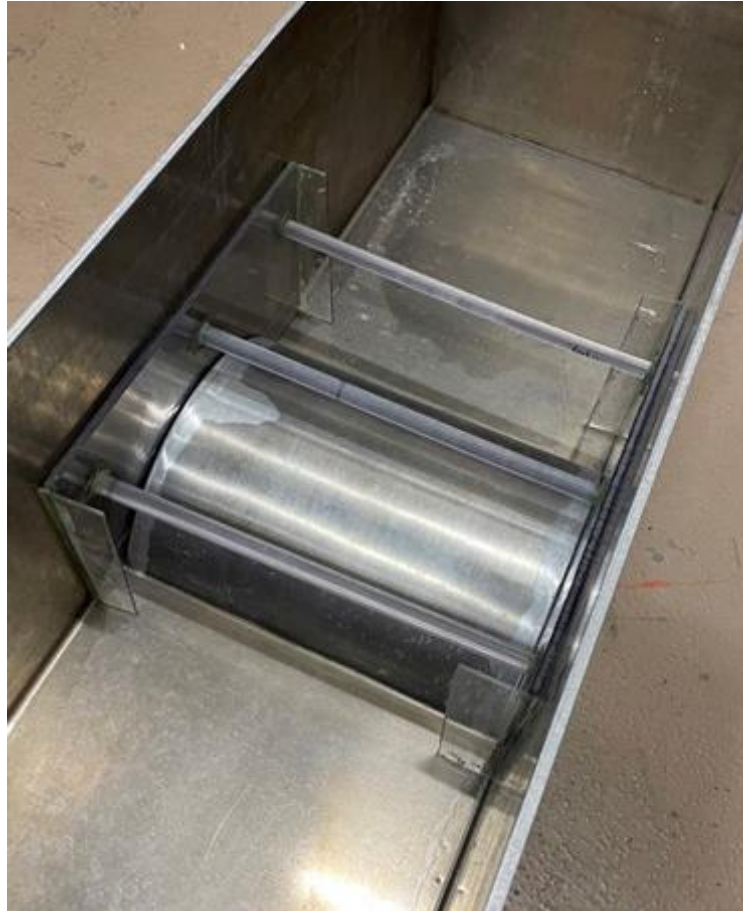
Figure 18: Polycarbonate structure in ice mold.

- Warm water tank: Free ice block from metal box. The wooden box is oversized (48" length x 20" width x 24" depth) to easily fit the welded box (Figure 19). A water depth of half the height of the metal box (5") is needed to cover the entire outside depth of the metal box with warm water. The tank is sealed with a plastic liner (polyethylene, general-purpose wall barrier film; thickness: 0.35 mm). To drain the tank, the plastic liner is removed and water flows through a hole (1" diameter) in the bottom.

Figure 19: Warm water tank lined with plastic to loosen ice from welded box.

- Hoist on supported sliding beam: Lift ice blocks into warm water tank and flume by attaching onto hook frozen in ice block. The Buffalo Tools (St. Louis, MO) electric cable hoist with wired control switch (EHOISTUL; 440 lb. capacity) (Figure 20a) is connected to a C-channel beam (Figure 20b), which is supported by posts on each side (Figure 20c).
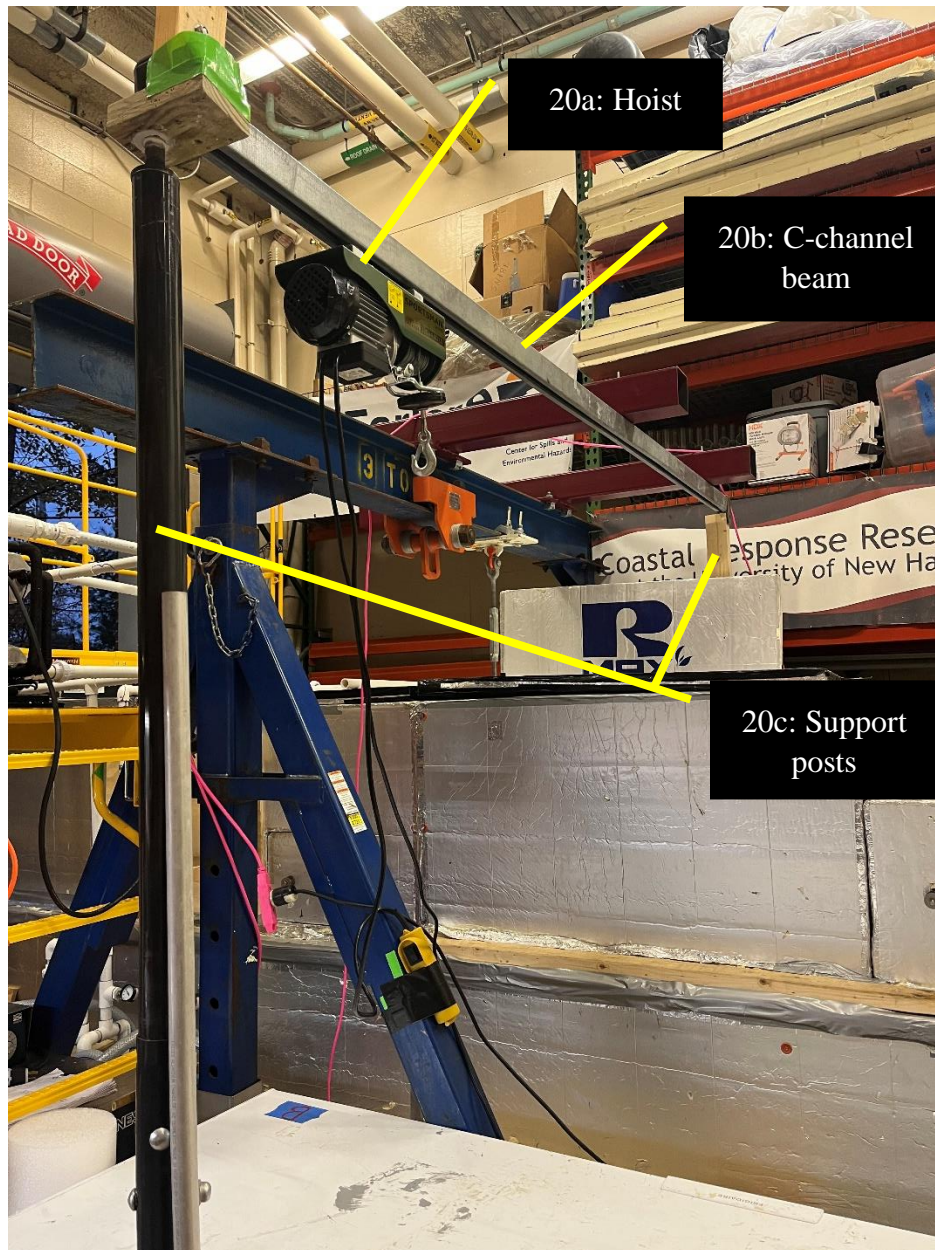
Figure 20: Hoist on sliding beam with support posts.

- Oil injection apparatus: Inject known volume of oil into cavity under ice. A peristaltic pump (Barnant Co.; 7523-40; Barrington, IL; capacity: 10-600 rpm) (Figure 21a) has a uniform injection rate (e.g., 800 L/min with fresh HOOPS oil at -2°C). The oil travels from a jar (Figure 21b) through Masterflex Norprene food tubing (Cole-Parmer Instrument Co.; 06402-15; Vernon Hills, IL; ID: 3/16", OD: 3/8") (Figure 21c) that is connected to the tool that places the end of the tubing below the cavity (Figure 21d). The mass of the jar and tubing are determined using a balance (OHAUS NVT10201; Parsippany, NJ) before and after injection to calculate the oil discharged into the cavity (Appendix D).
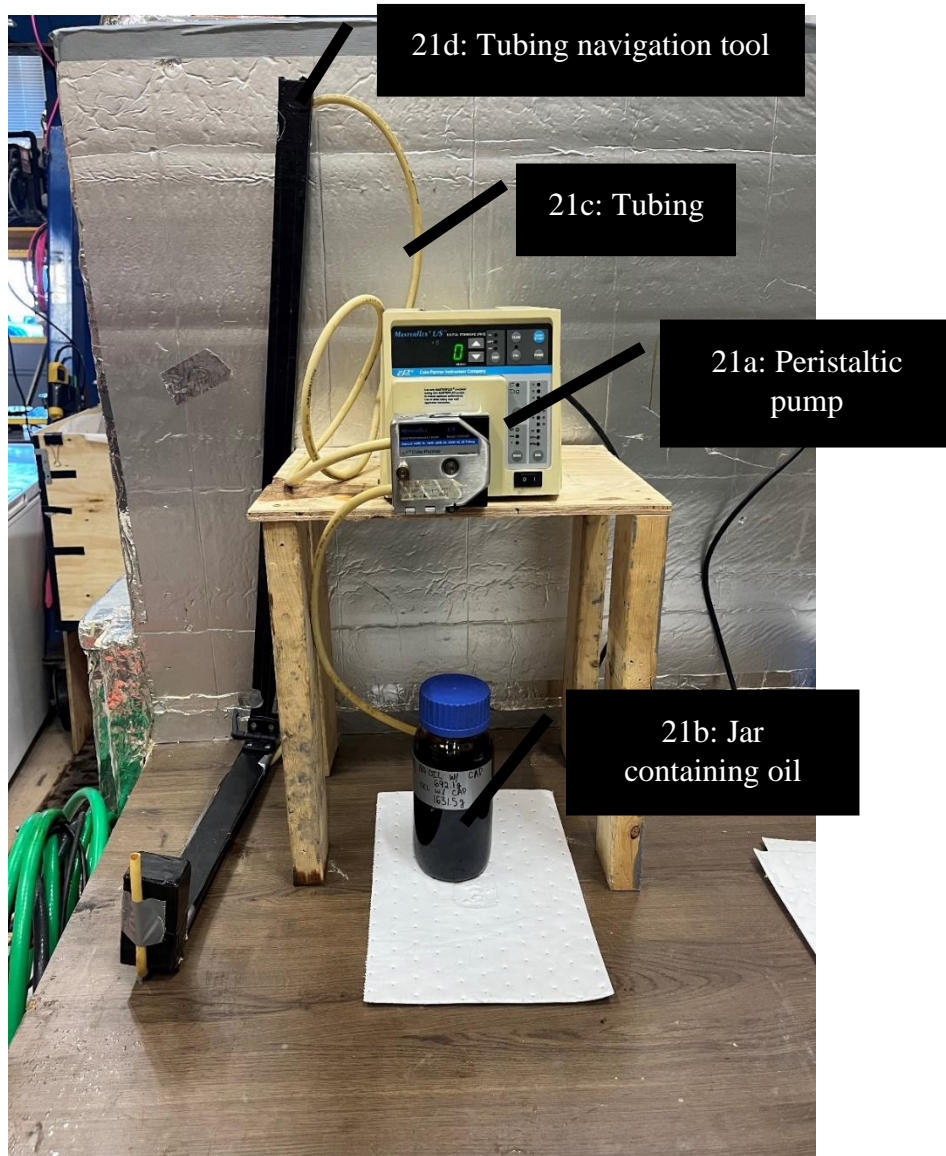
Figure 21: Peristaltic pump, tubing, and tool used for injecting oil into ice cavity.

- Fresh (non-weathered) HOOPS crude oil (sourced from Bureau of Safety and Environmental Enforcement (BSEE) Ohmsett Facility in Leonardo, NJ): Injected into cavity for experiments.

- Vectrino (Nortek AS; Rub, Norway; Vectrino Profiler Fixed Prove 10MHz, P 26301; Probe ID: VCN 9243; Hardware ID: VNO 1373): Measure relative velocity in x, y, z directions (Figure 22a) from its designated stand (Figure 22b). Per manufacturer's instructions, 20 grams of kaolinite clay (approximately 0.00764 g/L) is suspended in the water column to provide neutrally buoyant particles in the water which generate a stronger acoustic signal in the water. A rubber mat (1/4" thickness; Grainger; BULK-RS-RCY60-36) (Figure 22c) is placed along the flume bottom to decrease signal reflectance per manufacturer's recommendation.
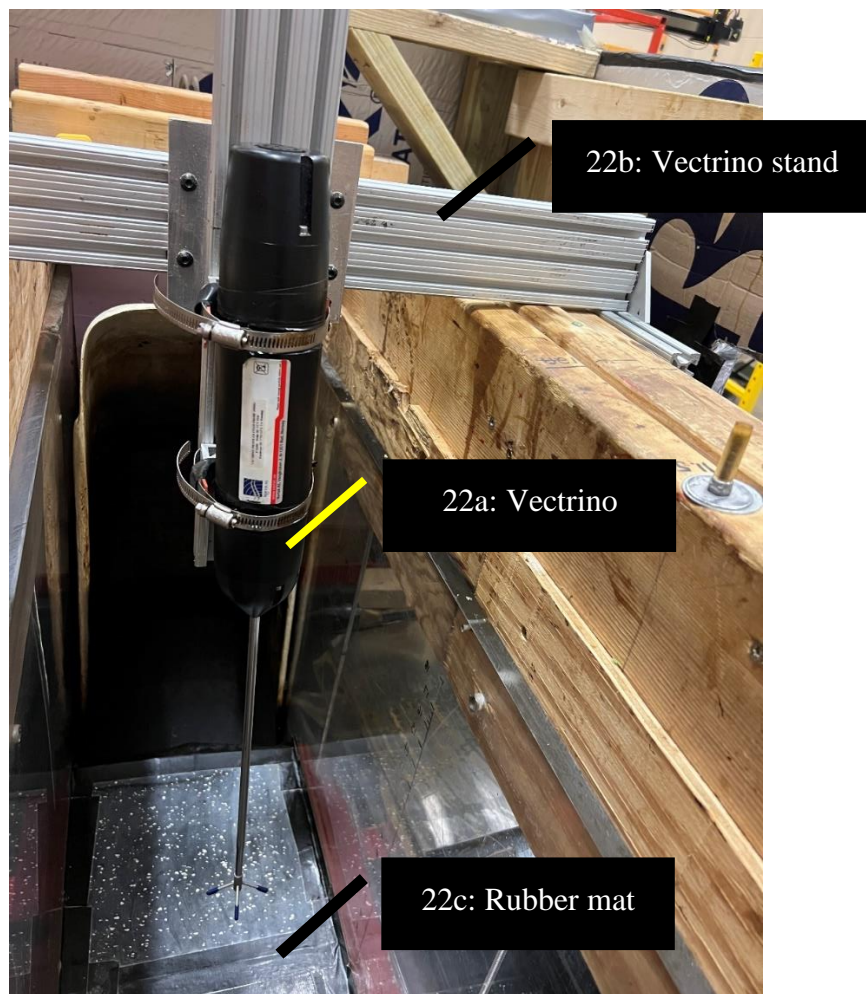
Figure 22: Vectrino secured to stand in flume.

- Mirrors (optional): View underside of ice throughout experiment.

- GoPro cameras (GoPro, Inc. Woodman Labs, Inc.; San Mateo, CA): Record experiment from three different positions: side view of ice cavity (Figure 23), 3-dimensional view including downstream end of ice cavity and underside of ice (Figure 24), and an upward looking view focused on oil in cavity (Figure 25). Two Hero 8 Black models are used for the 3-dimensional and upward views (CHDHX-802-XX/802-RW/802-TH) and one Hero 4 model for the side view (HWBD1 CHDHY-401). The lights along the outer length of the flume are flashed 2-3 times to indicate relative velocity changes in the videos throughout the experiment.
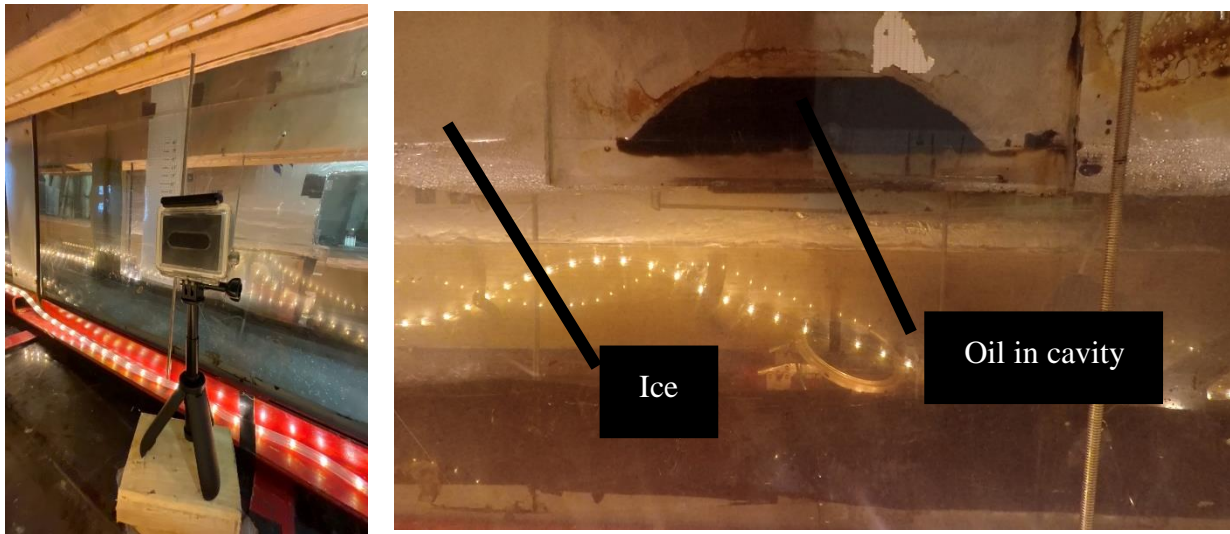
Figure 23: GoPro camera and its side view of ice cavity.

Figure 24: GoPro camera and its 3-dimensional view including downstream end of ice cavity and underside of ice.

Figure 25: GoPro camera and its upward looking view focused on oil in cavity.

4. Methods

At the start of this project, a scientific advisory committee of the following experts was formed:

- Chris Barker (NOAA Office of Response and Restoration (OR&R))

- Kelsey Frazier (Ted Stevens Center for Arctic Security Studies)

- Debbie French-McCay (RPS Group)

- Melissa Gloekler (RPS Group)

- Amy MacFadyen (NOAA OR&R)

- Ted Maksym (Woods Hole Oceanographic Institution)

- Marc Oggier (University of Alaska Fairbanks)

- Scott Socolofsky (Texas A&M)

- Jeremy Wilkinson (British Antarctic Survey)

They provided expertise on Arctic sea ice and oil spill response and the kinds of environmental conditions and data that would be beneficial to incorporate into trajectory models. They guided protocol design and recommended materials to obtain the data needed to improve under ice oil spill trajectory modeling, including ice cavity size and shape.

For this research, initial experiments were conducted to develop a protocol for conducting experiments on oil movement under ice and preliminary data was collected. The thesis research consisted of three goals:

1. Replicate Arctic conditions.

2. Freeze ice blocks to specified shape and secure in flume.

3. Develop a repeatable experimental protocol to monitor the behavior of oil under ice.

4.1 Replicate Arctic Conditions

Replication of Arctic conditions was accomplished by upgrading the existing flume to accommodate cold water operations. The flume was insulated to thermally isolate it from ambient room conditions. The insulation was attached to a wooden frame built around the flume with a minimal footprint to conserve lab space. Loads were distributed to the floor, rather than onto the flume to prevent damage. Sections of the insulation had to be easily removed for setup and cleaning. An air conditioner was installed to cool the air between the flume and insulation. Four water chillers were plumbed into the flume. Upstream flume water was pumped through one of two heat exchangers, each connected to a closed loop chiller, and then through one of two open loop water chillers. The chilled water was distributed downstream in the flume (Figure 12). The exchangers transfer heat from the flume water to water that runs through closed loop water chillers. The flow in the flume must be turned to a low setting (0.20 m/s; 2.0 Hz) to continuously mix the water for uniform chilling. Anti-fog (Rain-X 630046; Memphis, TN) was used on the outside of the clear acrylic flume walls to prevent condensation from obstructing the view of the experiment. The standard operating procedure (SOP) to chill the flume is in Appendix A. The water in the flume is chilled to 4℃ before running an experiment. This is the most achievable temperature which decreases the melting rate of the ice to allow time for an experiment to be completed. A lower water temperature may be reached by operating the chilling system for a longer period and using seawater which has a lower freezing point.

4.2 Freeze Ice Blocks to Specified Shape and Secure in Flume

Prior to starting an experiment, a flat ice block and an ice block with a cavity must be

frozen beforehand. To create an ice block with a cavity, a mold that can withstand the pressure of

water freezing must be constructed and sealed within a liner that can be removed from the ice.

There were several iterations of molds to make the ice blocks. Initially, wooden boxes were built

with reinforced, collapsible sides (Figure 26). Sides were reinforced with wooden ribbing to

prevent bowing from the pressure of water freezing. Hinges were placed along the bottom to fold

the sides down when removing the ice block (Figure 27). This design was simple and provided

the structure needed to freeze water into customized ice blocks.

Figure 26: Wooden box for ice block.

Figure 27: Wooden box for ice block with sides collapsed.

A wooden structure with a hook was strapped on top of the ice block to lift it from the freezer with a hoist (Figure 28).
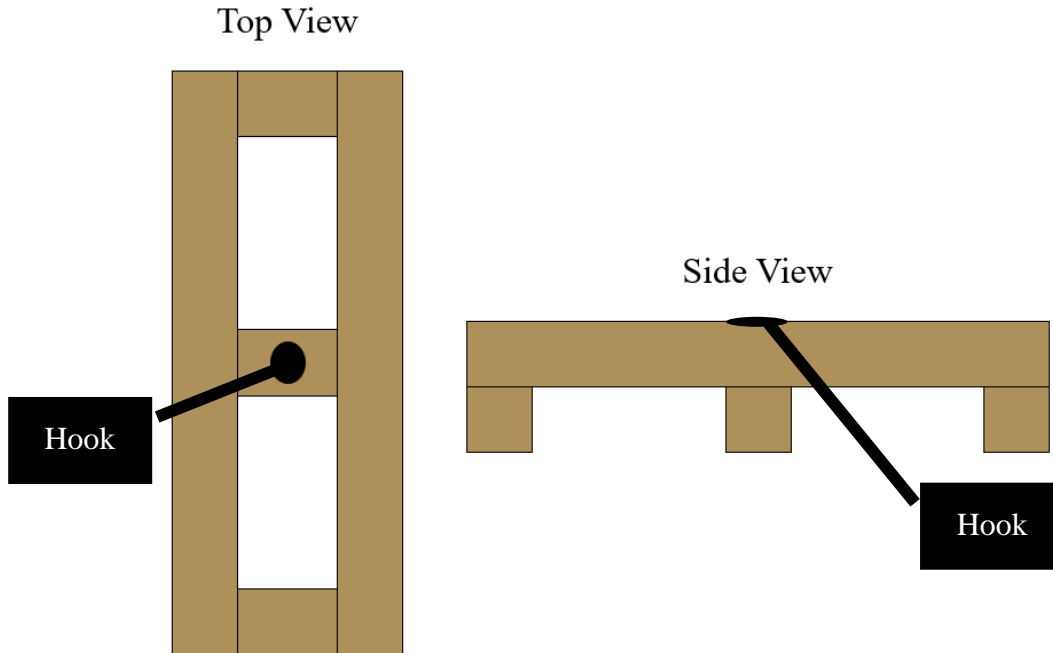
Figure 28: Top wooden structure to lift ice block.

Straps were secured under the bottom of the box, around the ice block, and tightened on the top wooden structure. The sides of the box were collapsed, and a hoist lifted the ice block via the hook in the top wooden structure, with its wooden bottom attached. The wooden bottom remained attached while the ice block was lifted to provide stability and hold the ice block in the straps. Once the ice block was placed in the flume, then the straps were released from the hoist and the wooden bottom and top could be removed. This apparatus filled about 4" in vertical distance more than the thickness of the ice block because of the wooden support bottom and top wooden structure. The distance between the hoist and the top of the flume is only 15", so maneuvering was difficult. Removing the board from beneath the ice block was also clumsy. Therefore, fiberglass rebar with a hook secured to its top was frozen into the ice blocks to provide a support structure from which to lift the ice block (Figure 16).

Rope is frozen into the ice to suspend the rebar from the bottom of the ice block bottom while it is freezing. The rope is also used to secure the ice blocks in the flume by tying it to bolts on the flume. Initially, magnets were used to hold the two ice blocks together, but these did not stay in place as soon as the ice began melting. The ropes alone hold the ice in place and prevent ice movement, so no other accommodations are needed. Velocity of the secured ice is assumed to be zero in all directions.

There were also challenges in sealing the wooden box so it could hold water. Initially, Teflon sheeting was used to line the wooden box, and its corners were folded and taped flat (Figure 29). To remove the ice blocks from the box, the sides collapsed, and the liner was peeled away from the ice blocks. However, the Teflon ripped easily, the ice would freeze around wrinkles in the liner, making it hard to remove without cutting it. It was not practical to retape the cut liners each time.
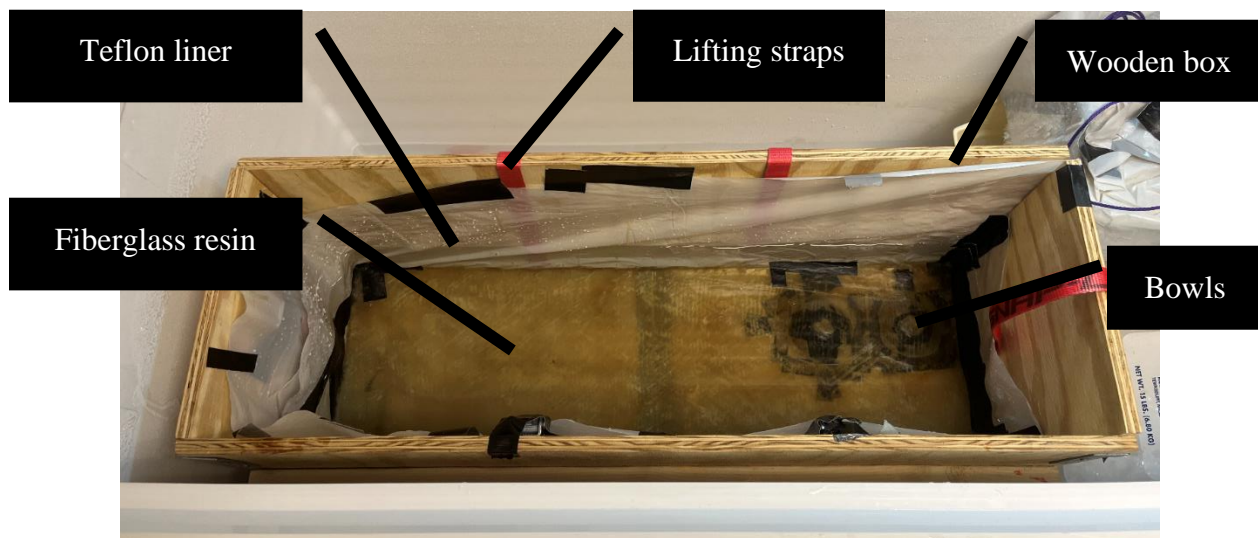
Figure 29: Wooden box with bowls sealed into the Teflon liner using fiberglass resin. The Teflon wrinkles froze into the ice block, so the liner could not be removed. Lifting straps were secured around removable wooden bottom. The wooden bottom imposed height restrictions.

Next, pieces of aluminum flashing were used as a liner and different adhesives were tested (i.e., fiberglass resin, silicone, metal bonding glue) to make it watertight (Figure 30). To remove the ice blocks from the box, the ice block and aluminum flashing liner were hoisted into a warm water tank to slightly melt the sides of the ice block and loosen it from the liner.
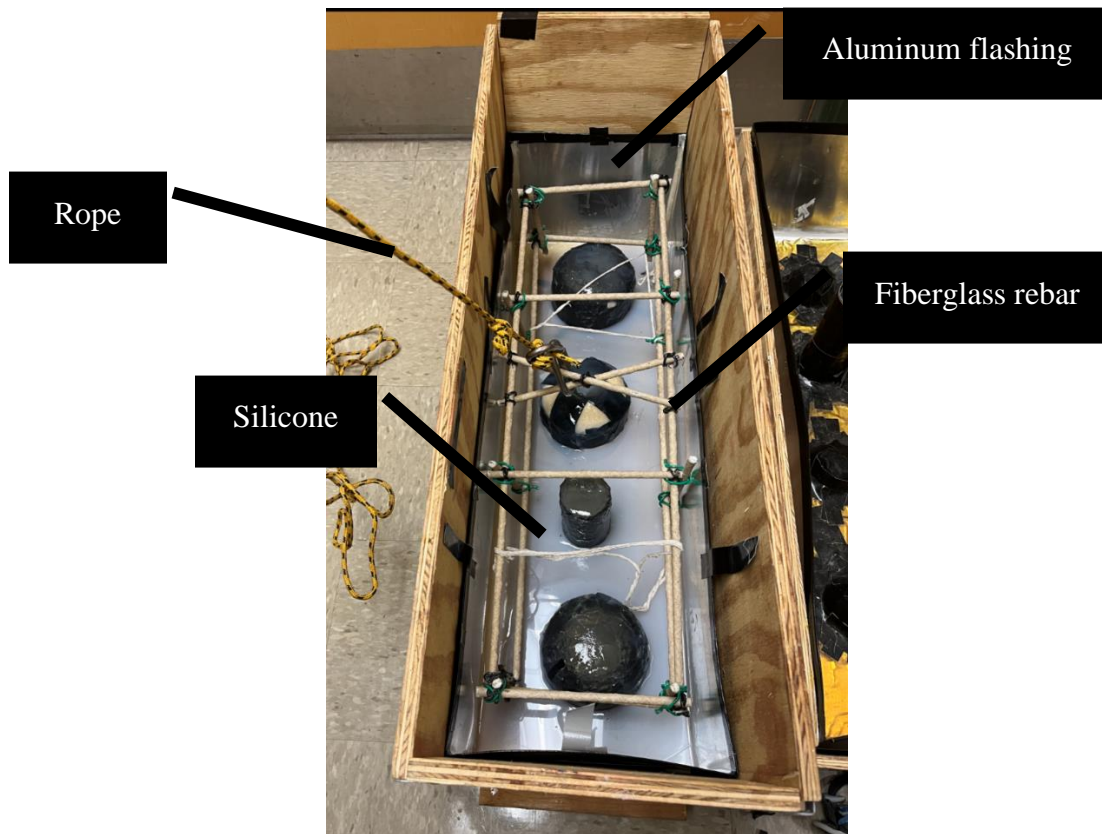
Figure 30: Attempt using aluminum flashing liner sealed with silicone and fiberglass rebar structure. The fiberglass rebar structure proved to be an appropriate lifting mechanism. Rope suspended the rebar from the bottom of the ice block.

The adhesives were supposed to seal the molds within the liner so that the ice blocks could be easily removed and shaped with cavities. One adhesive used was fiberglass resin, but it cracked when removing the ice block from the mold and remain stuck to the ice block (Figure 31).

Figure 31: Fiberglass resin remained on bottom of ice block, as it snapped around molds (Styrofoam hemispheres).

Silicone adhesive was used, but it became stuck to the ice and as melting occurred it floated away in the water in the flume. A metal bonding glue (Surebond; St. Charles, IL) was used, but it was difficult to apply and would not hold together while the ice block was removed (Figure 32).

Figure 32: Attempt sealing aluminum flashing liner with metal bonding adhesive (dotted line), which was difficult to achieve and maintain a watertight seal. The liner was sealed along each bottom edge, along a side edge where the aluminum flashing overlapped, and along the edges of the mold.

Members of the advisory committee provided advice on shaping the ice block cavity based on influencing the flow for modeling purposes and probable environmental conditions. A cavity in the shape of a half cylinder allows the water to move across the surface of the oil in the direction of the flow (Figure 33). Initial hemisphere molds (Figures 29-31) caused oil to flow in circular motion within the ice cavity (Figure 34).
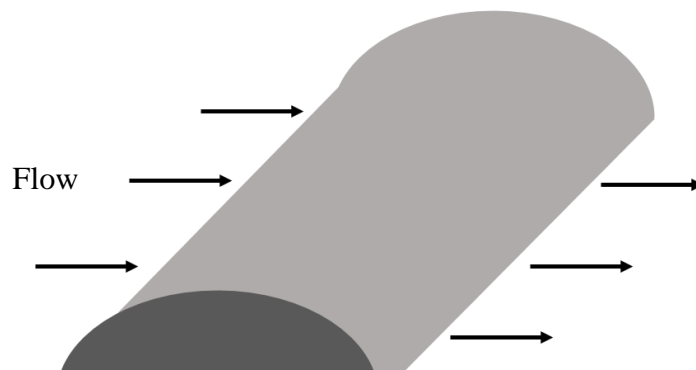
Figure 33: Flow across surface of half cylinder.
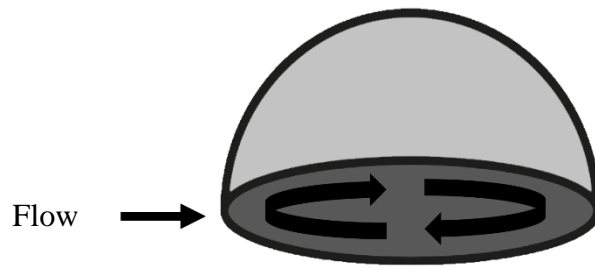
Figure 34: Flow across surface of hemisphere.

The half-cylindrical shape allows oil to seep out the sides laterally (perpendicular to flow) and migrate towards the water surface, instead of being contained in the cavity. To prevent this oil movement, acrylic pieces were frozen into the ice along the sides of the cavity. However, acrylic snapped easily while maneuvering the ice block into the flume. Thin ice could also snap and melt rapidly. A stronger material, polycarbonate, was necessary to prevent the unwanted oil movement out of the cavity. A radius was carved into the bottom of the polycarbonate sheets to fit tightly against the weld in the ice box. The two polycarbonate sheets are held in place with glued polycarbonate rods. Additional pieces along the edges of the polycarbonate protrude an inch into the ice blocks (Figure 17). Without the additional pieces along the polycarbonate edges that protrude into the ice, oil seeps out along the edge of the polycarbonate and migrates towards the water surface.

The section of the cylinder is elliptical because cavities under sea ice are more likely to have larger length than height. The length radius to height radius recommended by the advisory committee was 1.5:1, where the height radius is 3", and the length radius is 4.5" (Figure 35). This shape is based on probable conditions in the environment. An ice block with a uniform flat

surface is placed upstream of the ice block with the cavity to create a stable flow regime prior to the cavity.
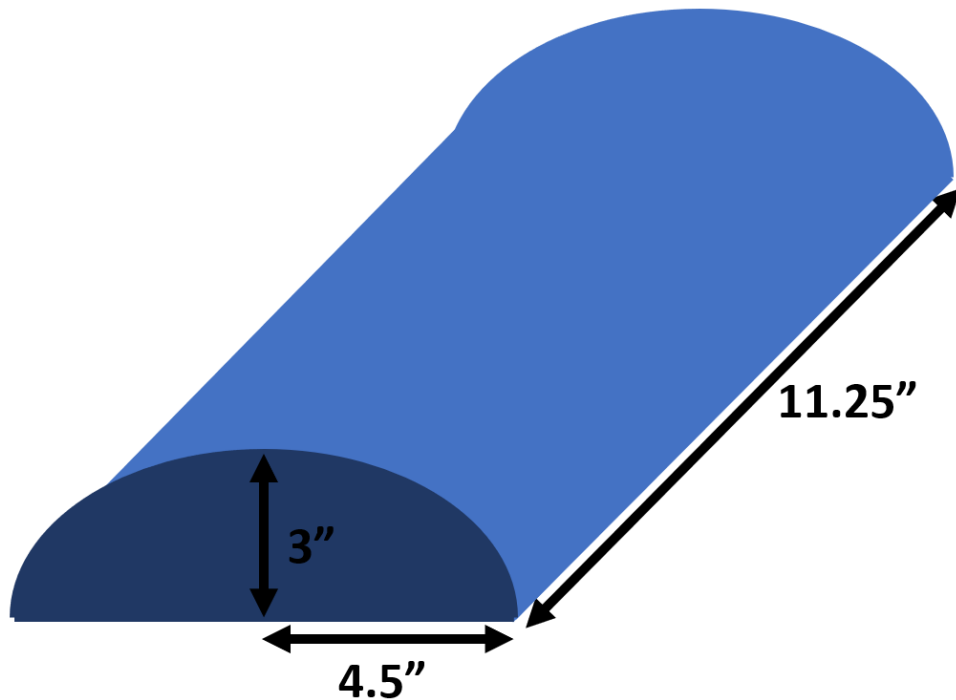
Figure 35: Ice mold shape.

Oil will displace water under the ice equal to its volume and reside in the cavity when there are no currents or waves present because its density is less than water and there is a buoyancy force (F_B, weight of displaced water) greater than the force due to gravity (F_G, weight of oil). There are also pressure distributions normal to oil from ice (F_{NI}) and water (F_{NW}) (Figure 36).
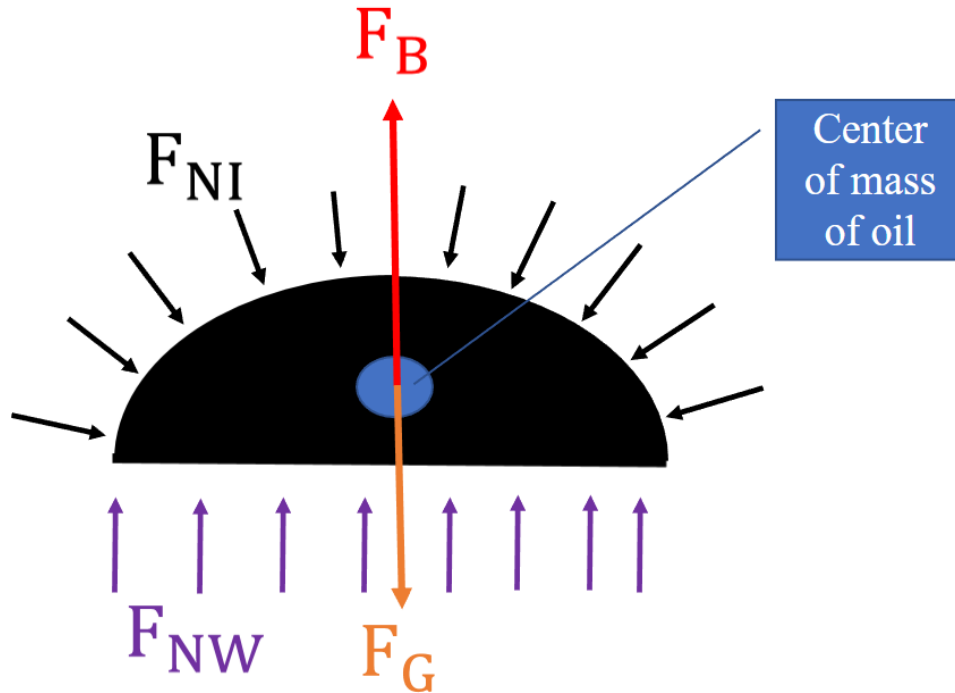
Figure 36: Free body diagram of oil full in ice cavity. F_B=buoyancy force; F_{NI}=pressure distribution normal to oil from ice; F_{NW}=pressure distribution normal to oil from water; F_G=force of gravity on oil

When there are currents or waves present, there are resultant shear forces of oil moving relative to water (F_{SW}, force tangential to oil and water interface related to viscosity and velocity profile of water) and relative to ice (F_{SI}, force tangential to oil and ice interface related to viscosity of velocity profile of oil) (Figure 37).
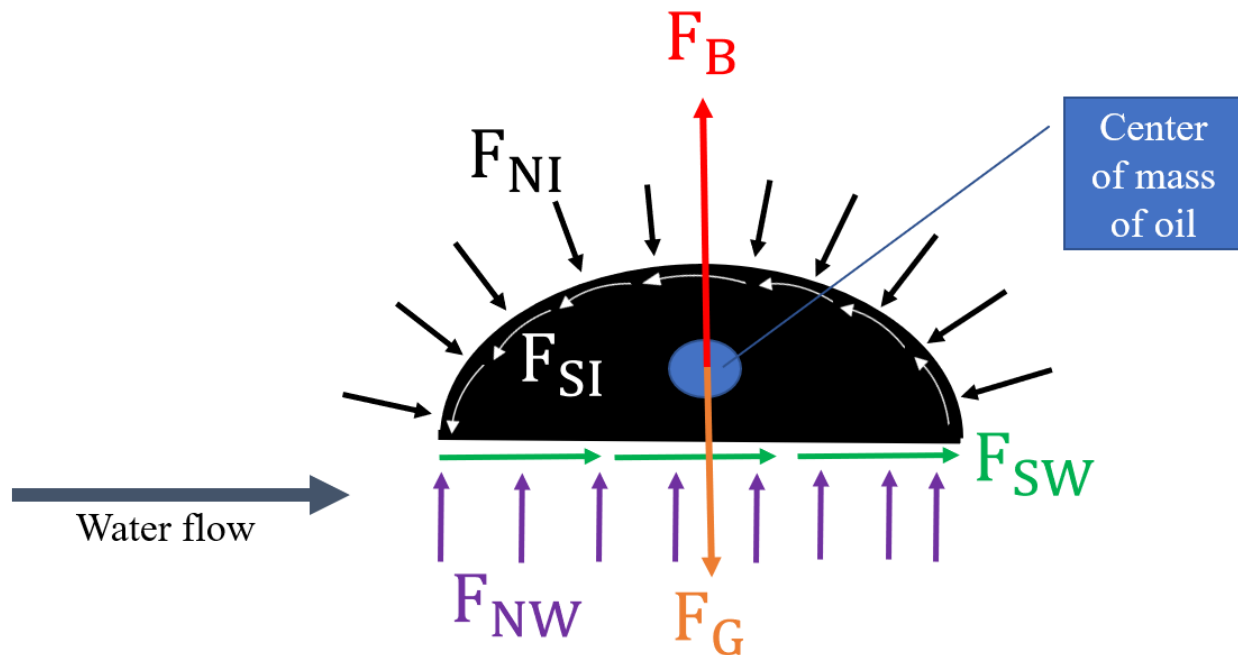
Figure 37: Free body diagram of oil full in ice cavity. F_B=buoyancy force; F_{NI}=pressure distribution normal to oil from ice; F_{SI}=resultant shear force of oil moving relative to ice; F_{NW}=pressure distribution normal to oil from water; F_G=force of gravity on oil; F_{SW}=resultant shear force of oil moving relative to water.

When the flume was operating, and oil was flush with the surface of the ice at the water interface, a portion of the oil was stripped out at a low relative velocity (<0.20 m/s). A decrease in percentage and depth of oil in the cavity (Figure 38) causes the velocity gradient within the remaining oil to increase, which increased the resultant shear force of oil relative to ice. As the depth of water increased, the velocity gradient over it decreased, along with the resultant shear force of oil relative to water. A reduced amount of oil in the same cavity requires an increased relative water velocity to increase resultant shear force of oil relative to water and mobilize the oil once its critical shear stress (CSS) is reached.
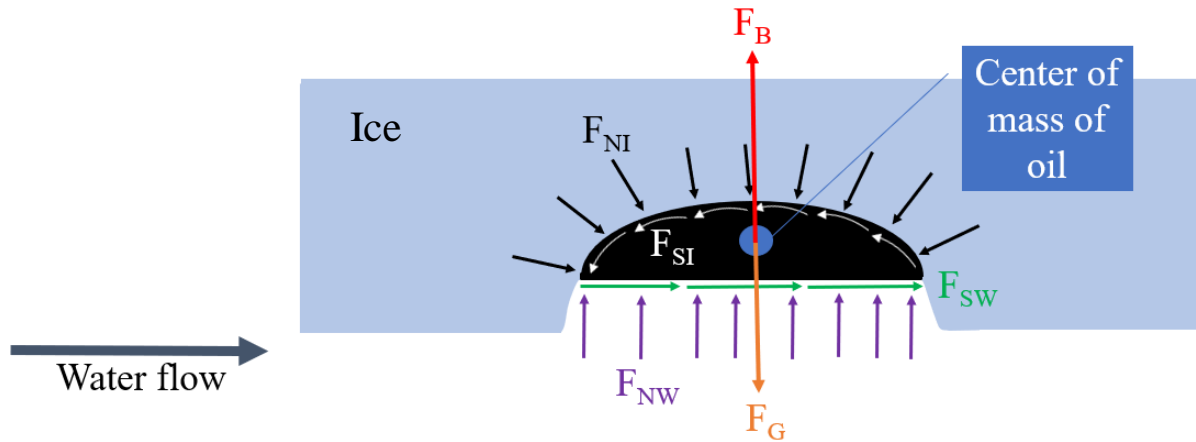
Figure 38: Free body diagram of decreased volume of oil in ice cavity. F_B=buoyancy force; F_{NI}=pressure distribution normal to oil from ice; F_{SI}=resultant shear force of oil moving relative to ice; F_{NW}=pressure distribution normal to oil from water; F_G=force of gravity on oil; F_{SW}=resultant shear force of oil moving relative to water.

The mold for the cavity was constructed using different materials. A 3D printer was assembled to shape the molds. However, it was time consuming to 3D print molds to the desired size. Shapes were also made using bowls or by shaping Styrofoam and wood. The bowls were not customizable, and the Styrofoam was difficult to shape and source in large blocks. Wooden sections were cut and lined with aluminum flashing (Figure 39), but the shapes were difficult to seal to the box and could not withstand the pressure from the water freezing above them (Figure 40).

Figure 39: Mold constructed with wooden sections and sealed with aluminum flashing.

Figure 40: Attempt shaping mold from wooden pieces sealed with aluminum flashing and metal

bond. Mold was not able to maintain its structural integrity from the pressure of the water

freezing.

Aluminum liners inside the wooden box had advantages (i.e., inexpensive to make, readily available, easily customizable, lightweight, constructed in-house), but they could not be made watertight. Prototype 1/4" aluminum welded boxed were made (Figure 14). These are: strong enough to withstand the pressure of water freezing, watertight, and can be reused without resealing. They are fabricated by a welding shop and cost $525 each. A set of boxes was made by Custom Sheet Metal (Manchester, NH); one flat bottom box and one with an elliptical cavity. The aluminum and smooth seams allowed for easy release of the ice from the box. Heat transfers quickly from the warm water tank through the aluminum to slightly melt the sides of the ice block to loosen it from the box (Figure 19). Appendix B contains the SOP to form ice blocks.

The advisory committee recommended use of freshwater in the flume. Seawater ice is difficult to make because salt will sink and form brine pockets and the freshwater on the surface will freeze first. The bottom of the block would remain as slushy ice due to its high salt content, which would deform the bottom of the ice and inside the cavity. The largest difference between freshwater and seawater ice in this application is likely the difference in permeability. Seawater ice has an increased permeability which could provide channels for oil to migrate upwards towards the surface.

4.3 Experimental Protocol

Once the ice blocks are frozen and the flume water is chilled, an experimental run can be setup and executed. This includes injecting a known volume of oil into the cavity, measuring temperature and relative velocity of the water under ice, and recording oil movement. The oil is chilled to -2°C in a freezer and flows from jars into the cavity using a peristaltic pump and Masterflex Norprene food tubing (Figure 21). The jars and tubing must be massed before and after the experiment to determine the residual oil (Appendix D). The density of the fresh HOOPS oil was determined using a hydrometer to be 0.881 g/mL at -2°C, and the volume injected into the cavity was calculated by the dividing the mass of oil injected by the density of oil.

After oil is injected into the ice cavity, the motors are started at 1.0 Hz and the propellors begin to turn and move the water. The flow of the water in the flume stabilizes within 15 seconds at 0.10 +/- 0.01 m/s. Relative velocity is increased in 0.08 +/- 0.02 m/s intervals. These measurements align with previous work conducted in the MacFarlane Flume (Gloekler, 2021). If oil droplets mobilize from the cavity, then the relative velocity is held constant until there is no further movement. The lowest starting relative velocity and interval changes are used to understand movement of the oil at a fine scale.

The Sunken Oil Transport Tool (SOTT) (Gloekler, 2021) was used to obtain a rough estimate of an expected water relative velocity where the oil could move. SOTT estimates that sunken heavy reformate would erode around 0.2 m/s on a fine silt bed (d50 = 0.0078 – 0.0156 mm) (Gloekler, 2021). The environmental conditions and oil used in SOTT were not representative of the ice experimental conditions but identified a rough starting relative velocity for the first run. Relative velocities were then adjusted based on observed erosions.

The relative velocity of the water under the ice is measured using a Vectrino Profiler II, an Acoustic Doppler Velocimeter (ADV), in its designated location (Figures 41 and 42). Throughout the experimental run, water temperature is recorded, and the movement of oil is captured on videos by three GoPro cameras with different views: looking upward into the cavity, side view of cavity, and a 3-dimensional view including downstream end of ice cavity and underside of ice (Figures 23-25). Appendix C describes the SOP for the experimental protocol.
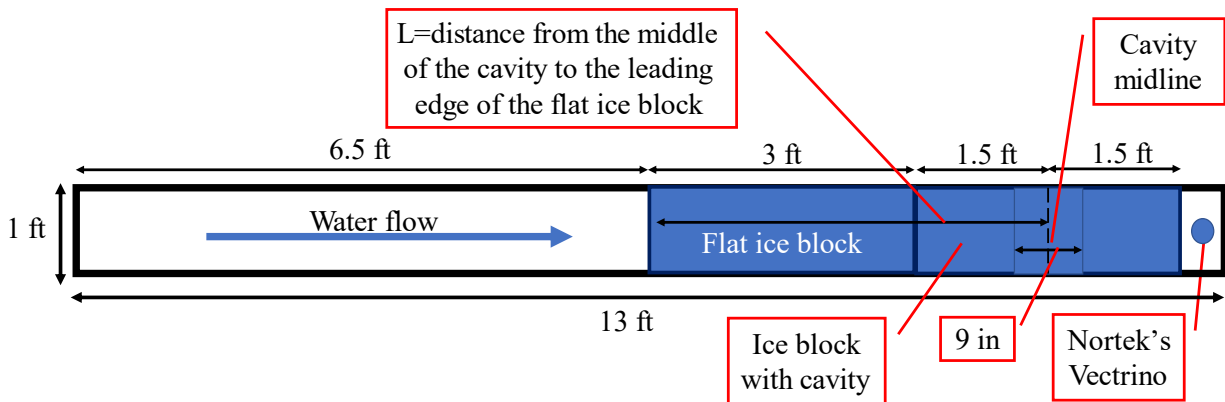
Figure 41: Plan view of experimental setup within flume top section.
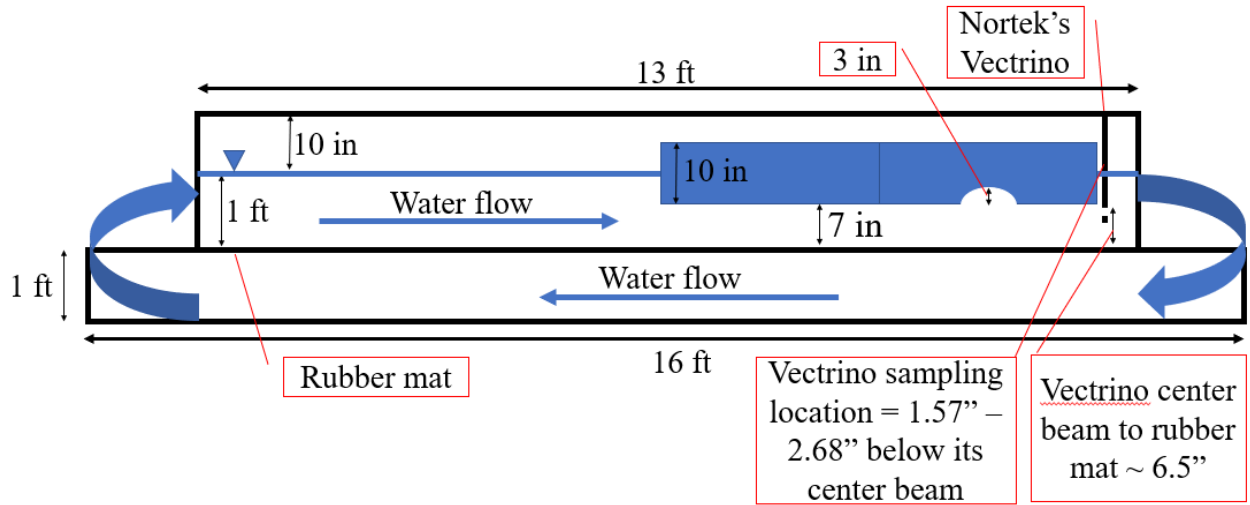
Figure 42: Longitudinal section view of experimental setup within flume.

5. Results and Discussion

The methods reported were developed to collect data for understanding the movement of oil under ice. The MacFarlane Flume was modified to simulate Arctic conditions by achieving a water temperature of 4°C prior to the start of experiments. Insulation helped maintain that water temperature. At 4°C, the ice blocks maintained their shape for ~1 hour. Methods were also developed to freeze ice blocks of specific dimensions and secure them in the flume. The size and shape of the cavity in the ice blocks (ellipse half cylinder across the span of the ice block width with a height radius of 3" and length radius of 4.5") was recommended by an advisory committee of sea ice and oil spill modeling experts. The protocols underwent several iterations until aluminum welded boxes were built to serve as molds for the ice blocks (Figure 43).
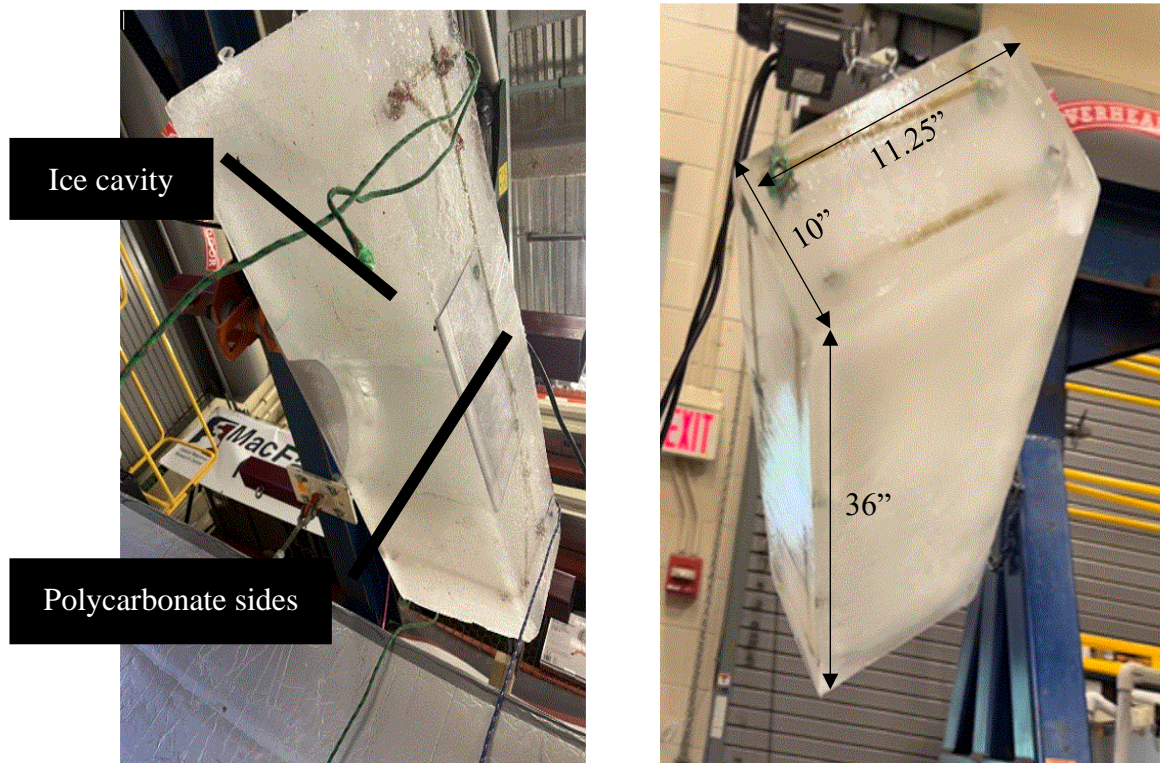
Figure 43: Ice blocks with and without a cavity.

A known volume of oil filled the ice cavity using the oil injection apparatus (Figure 21). The apparatus was positioned in the flume before the ice blocks. Oil was pumped from jars using a peristaltic pump and tubing navigated into the cavity (Figure 44). The apparatus was removed after the cavity was filled with oil and before the Vectrino was positioned in the flume. The mass of oil in the cavity was determined by measuring the mass of the oil jars and tubing before and after oil was injected. This was divided by the oil's density to determine the volume of oil in the cavity.
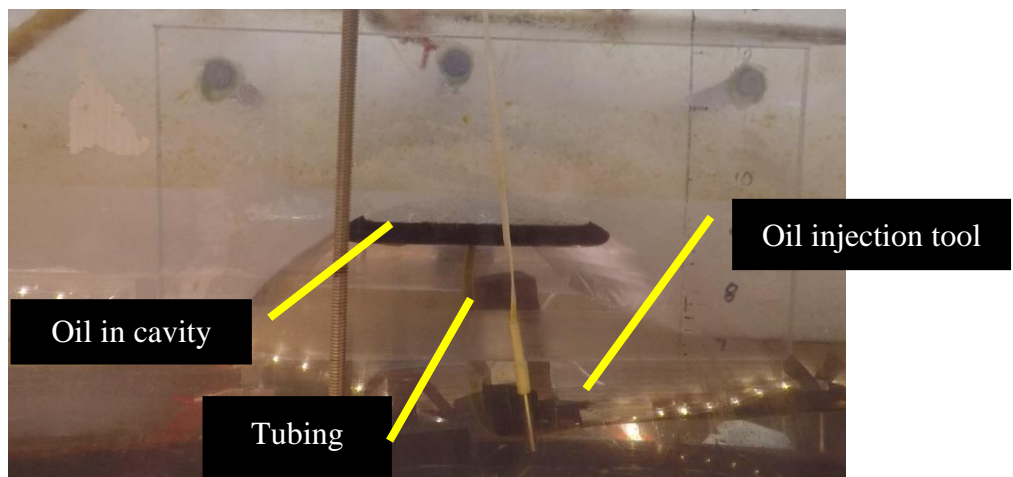
Figure 44: Oil injection tool filling ice cavity (side view).

Water temperature remained constant throughout each experimental run, which is important because oil viscosity is dependent on temperature. Relative velocity measurements using a Nortek Vectrino were validated through software analyses described below. Relative velocity patterns have been previously profiled in the MacFarlane Flume and correlated to motor settings (Gloekler, 2021). This provided a baseline with which to compare relative velocity measurements with ice blocks to those previously obtained, which validated that the velocimeter was functioning properly (Figure 45).
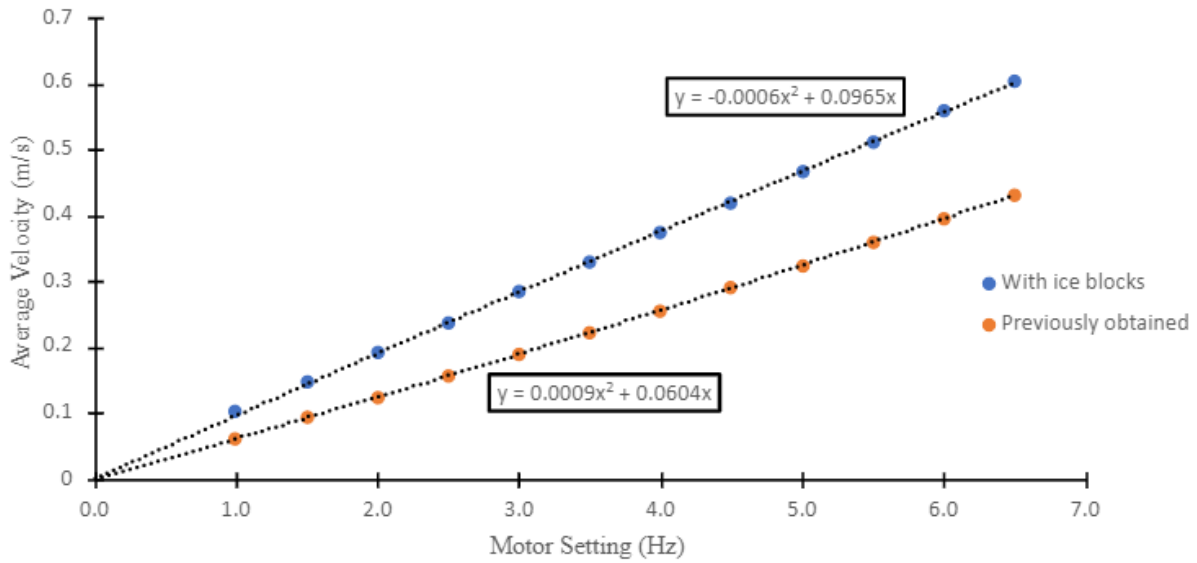
Figure 45: Average relative velocity (U) vs. motor setting (Gloekler, 2021).

The Vectrino Profiler software successfully reported the distance from the probe to a rubber surface on the flume bottom (approximately 17 cm). Also, it reported strong signal to noise ratio values (>10) (Figure 46), as well as correlation values (>70%) (Figure 47), as specified by the manufacturer (Nortek AS, 2018). The addition of 20 grams of kaolinite clay (approximately 0.00764 g/L) improved these readings because it increased the number of scatterers in the water column, which reflect sound pulses from the instrument to measure its movement.
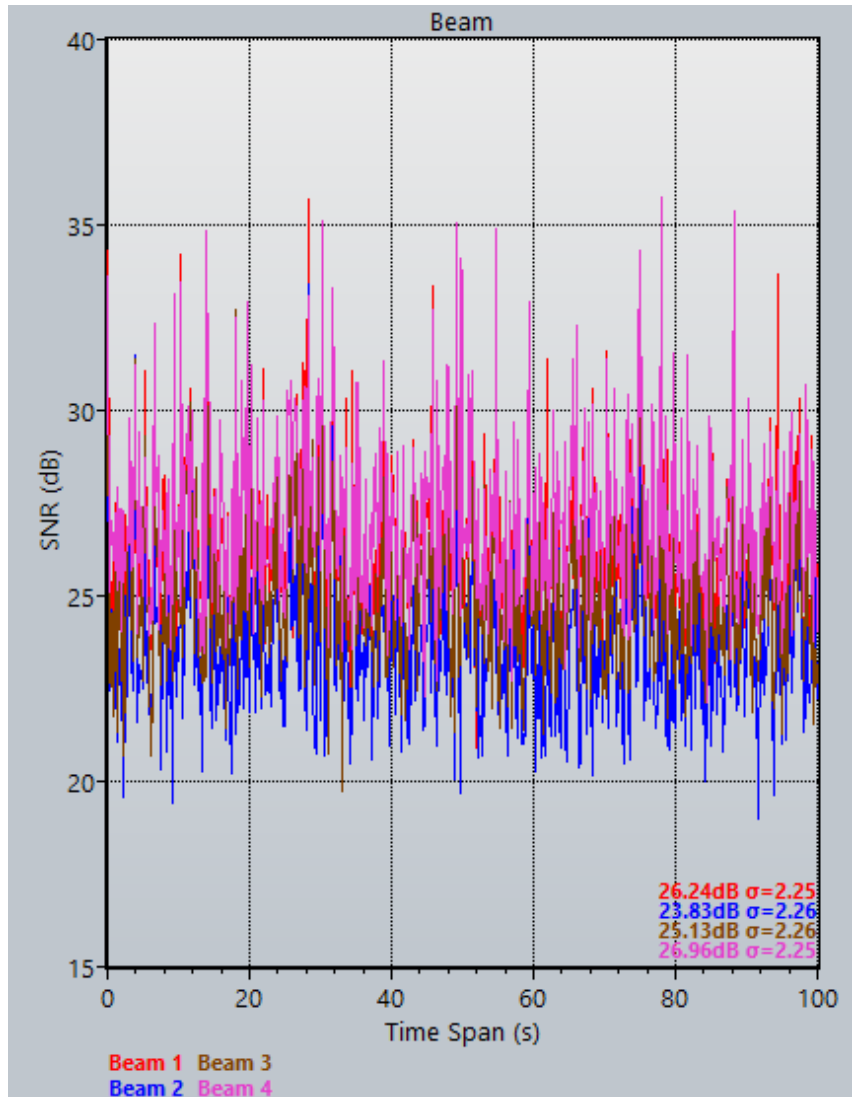
Figure 46: Vectrino Profiler shows strong signal to noise ratio over time. Manufacturer
recommended values of >10.
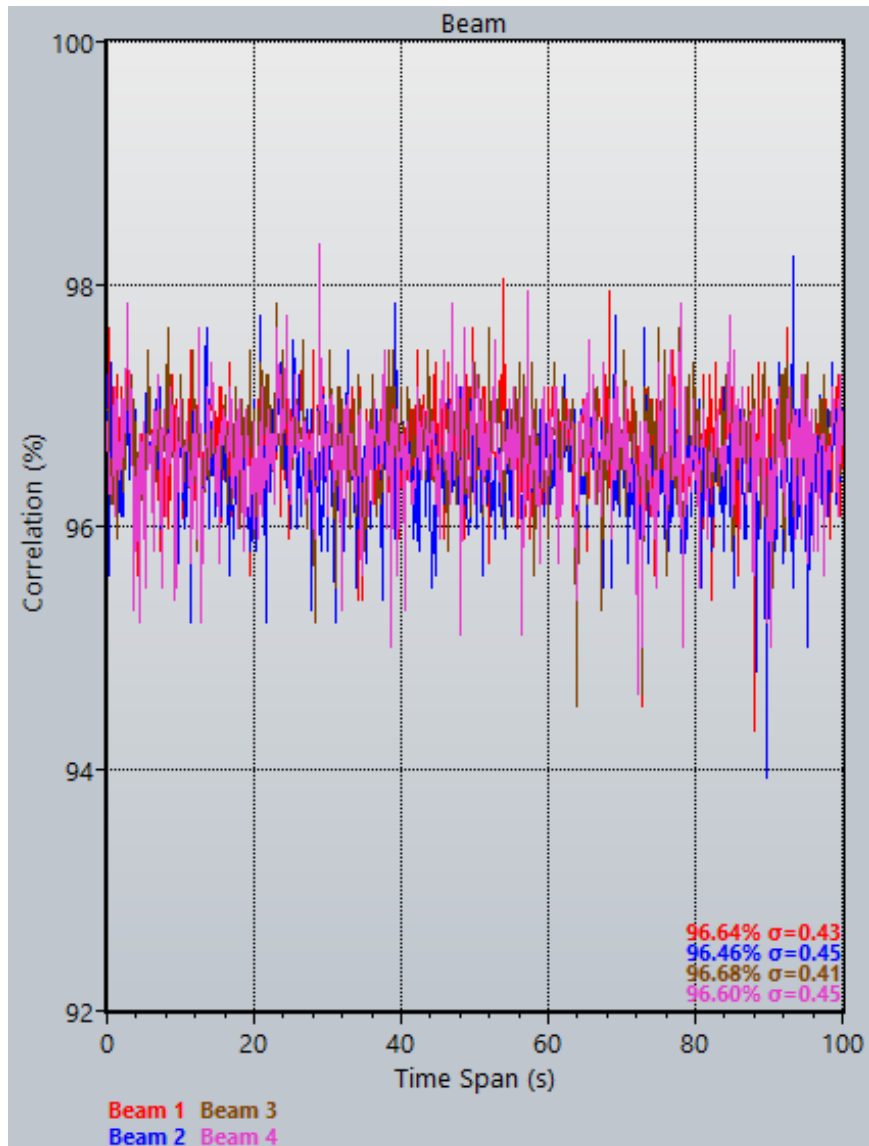
Figure 47: Vectrino Profiler shows strong correlation over time. Manufacturer recommended values of >70%.

Several parameters were controlled at the start of each experiment, including the following:

- Water temperature: 4°C

- Oil temperature upon injection (assumed minimal change throughout 60-minute experiment): -2°C

- Oil type and properties (e.g., viscosity, density): fresh HOOPS oil (density is 0.881 g/mL at -2°C, viscosity is about 23 cP at 5°C)

- Elliptical half cylinder ice cavity (9" length, 11.25" width, 3" height) (Figure 35)

- Oil volume: 100% of cavity (3,900 mL including volume of trapped air within cavity)

- Oil flowrate from jar into cavity: 800 mL/min

Oil erosions were classified applying a similar system used for sunken oil. For sunken oil, erosions are described as either gravity dispersion, rope formation, ripple formation, or break-apart/resuspension (Gloekler, 2021). These terms do not directly apply to floating oil moving under ice because the cavity contains the oil and prevents dispersion without a current present. A classification system was defined to describe the observed erosions of floating oil under ice and consists of ripple formation, edging blobs, droplet formation, and pod formation. Ripple formation occurs at the oil and water interface, while the oil is pooled within the cavity. The water currents cause rippling in the oil, but during this condition the oil remains within the cavity (Figure 48). Edging blobs occur at the downstream edge of the cavity. The oil slightly protrudes from the cavity, but sways back and remains associated with the mass of oil in the cavity (Figure 49). Droplet formation occurs when spherical oil droplets are released from the cavity (Figure

50). Pod formation occurs when a larger volume of oil is released from the cavity at once in an elliptical shape (length: width > 4) (Figure 51).
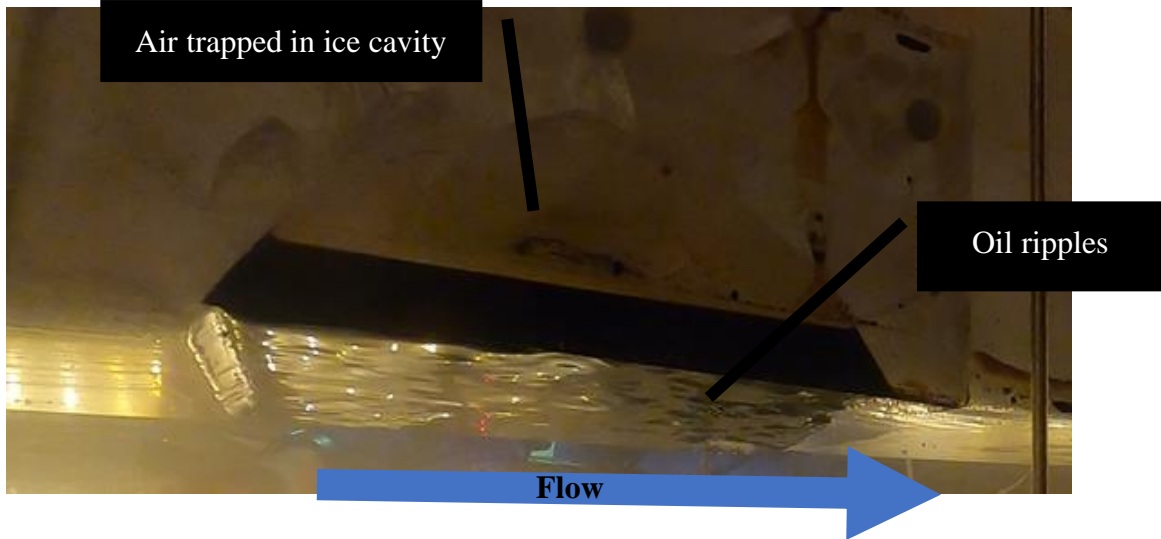
Figure 48: Oil ripple formation.
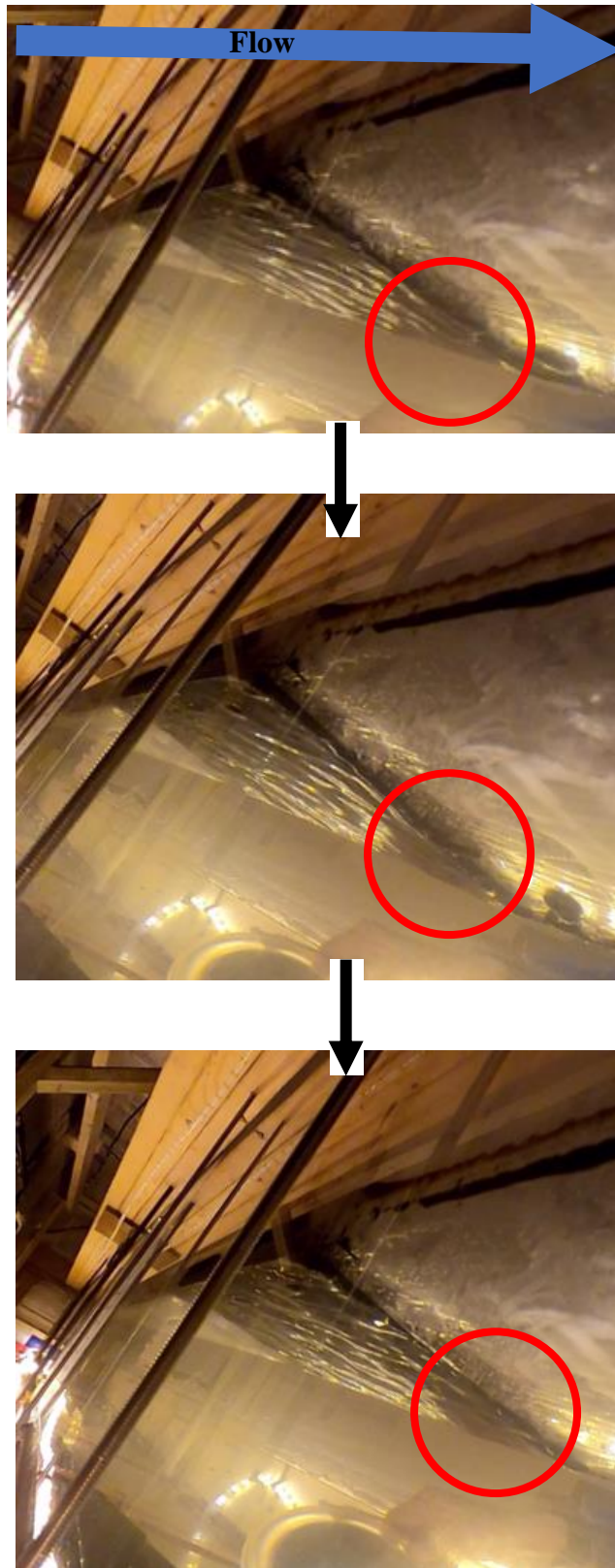
Figure 49: Edging blob formation.
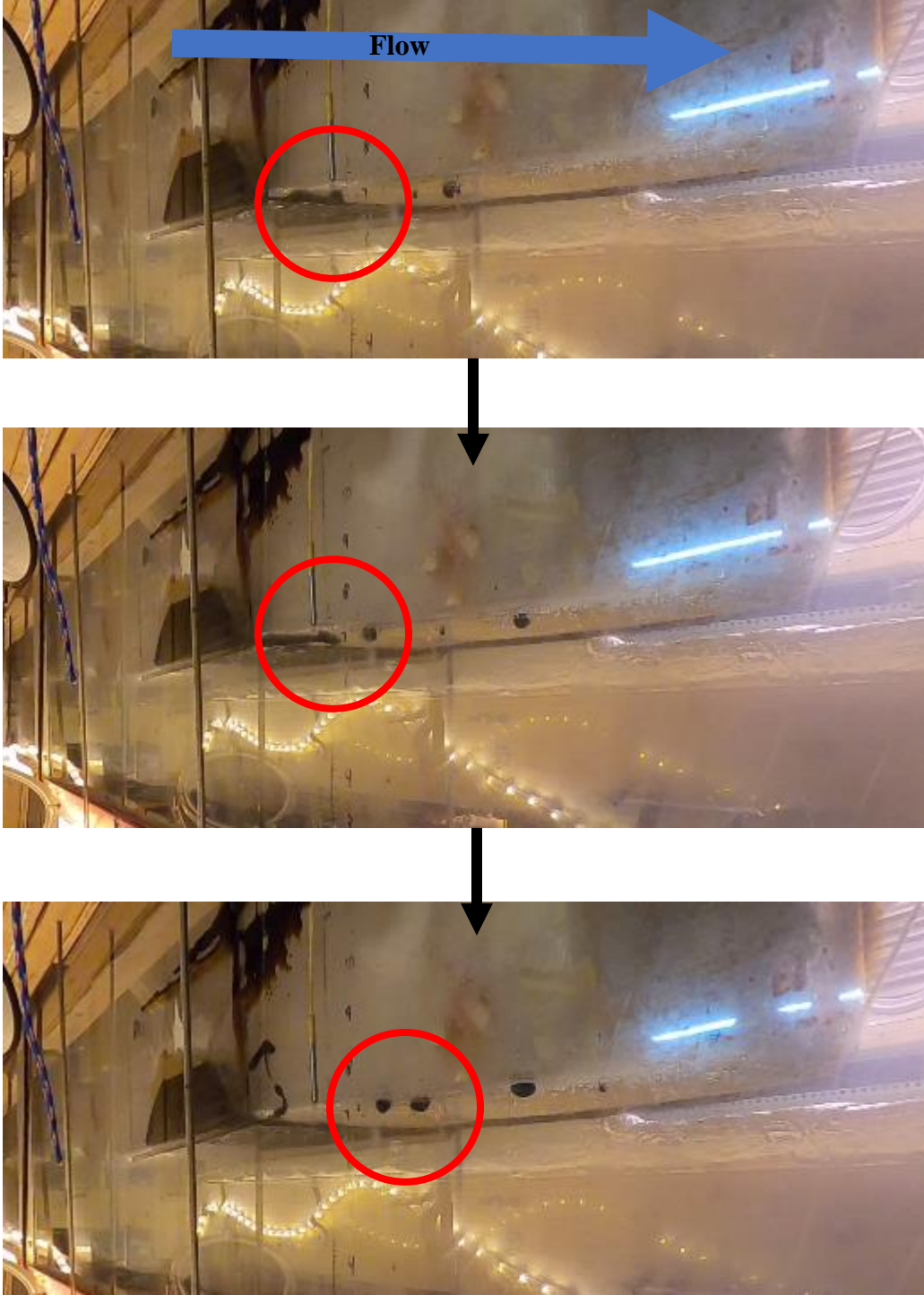
Figure 50: Oil droplet formation.

Figure 51: Oil pod formation.

Three experimental runs were completed starting with the cavity full of HOOPS oil and yielded similar results. For the first two runs, the motors for the flume propellors were initially set to the lowest motor setting, 1.0 Hz, which corresponded to a water relative velocity of 0.11 +/- 0.01 m/s for the first run, and 0.10 +/- 0.01 m/s for the second run. A previous protocol for studying sunken oil movement on sediment beds increased water relative velocity every 15 minutes (Gloekler, 2021). To decrease the time for ice melt, the motors for the flume propellors were increased after 10 minutes to 2.0 Hz in each run, which corresponded to a water relative velocity of 0.22 +/- 0.01 m/s for the first run, and 0.20 +/- 0.01 m/s in the second run. Future runs modified times intervals to further decrease ice melt. Ripple formation occurred and the oil remained in the cavity for both runs at 0.11 +/- 0.01 m/s and 0.10 +/- 0.01 m/s. Droplets were stripped from the mass of oil in the cavity at 0.22 +/- 0.02 m/s (Figure 52) and 0.20 +/- 0.01 m/s (Figure 53).
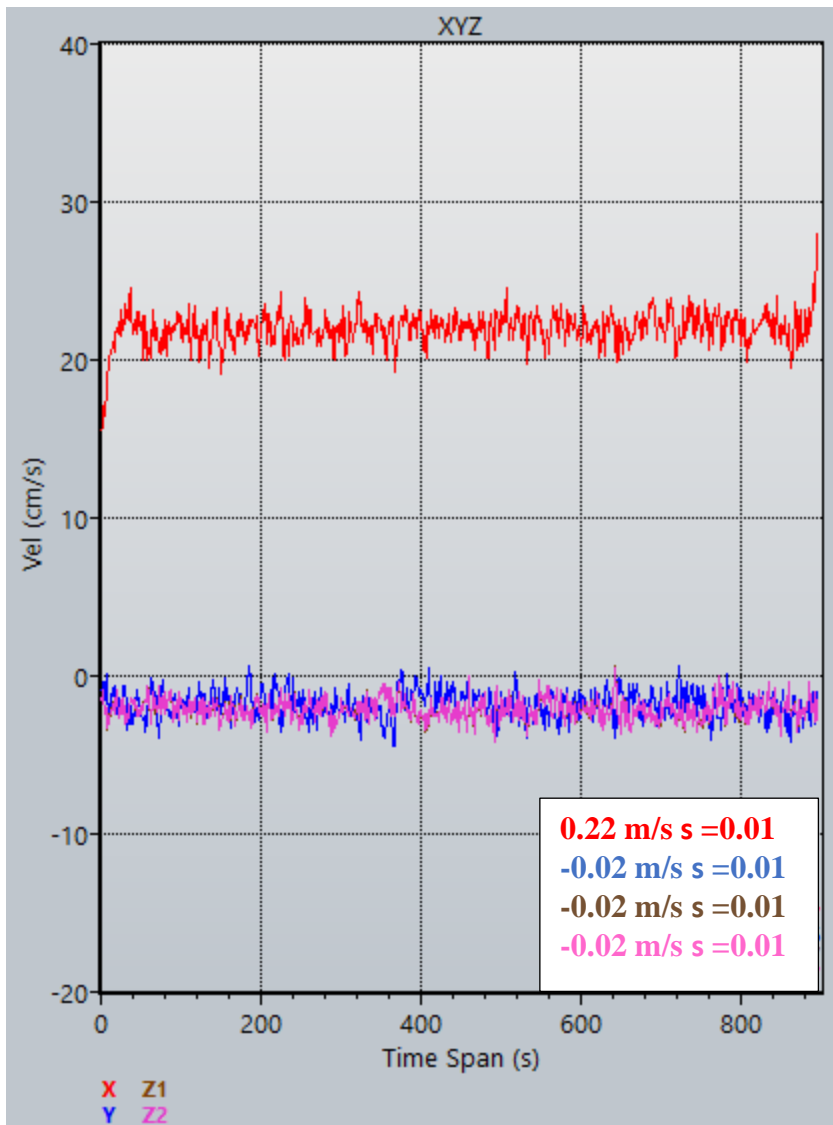
Figure 52: Run 1: relative velocity vs. time when oil was stripped from cavity.
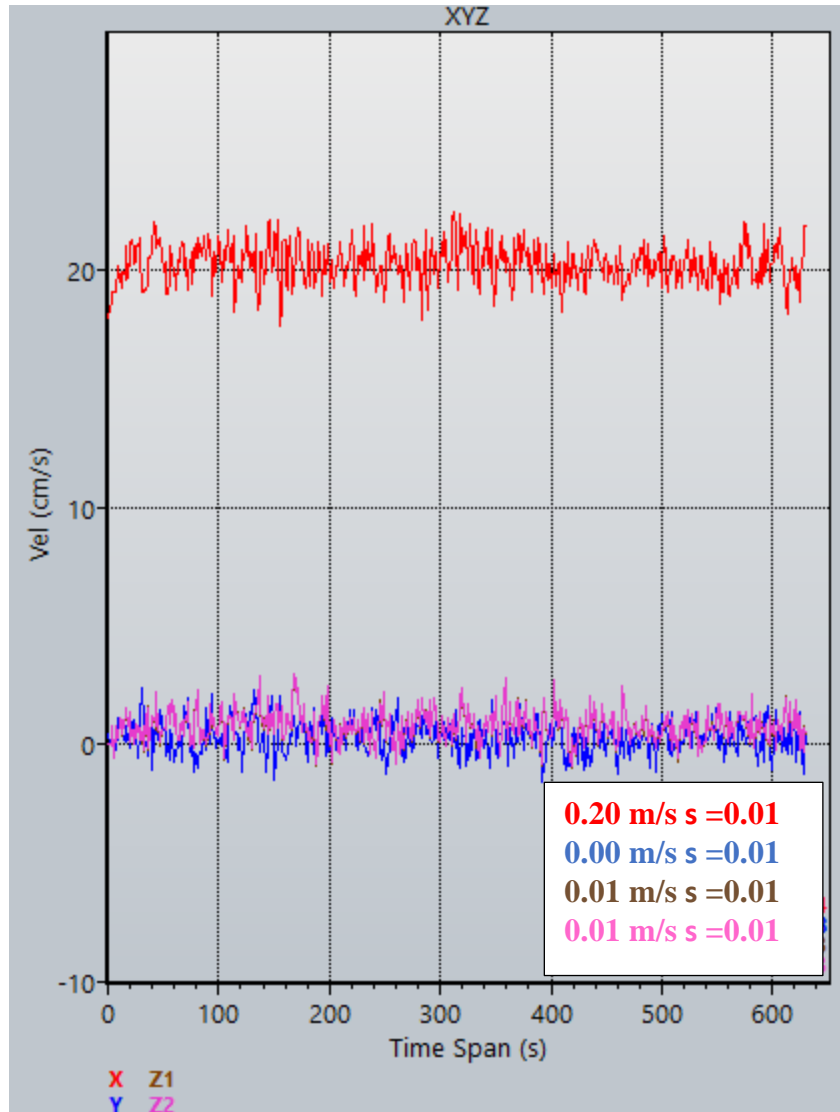
Figure 53: Run 2: relative velocity vs time when oil was stripped from cavity.

Data collection ended when significant ice melt was evident, and the oil and water had eroded paths in the ice that influenced oil movement. Examples of this observation used for initial trials are demonstrated in the snapshots below (Figures 54 and 55). Future runs should end once the ice block has been in the water for 20 minutes for a more definitive protocol.
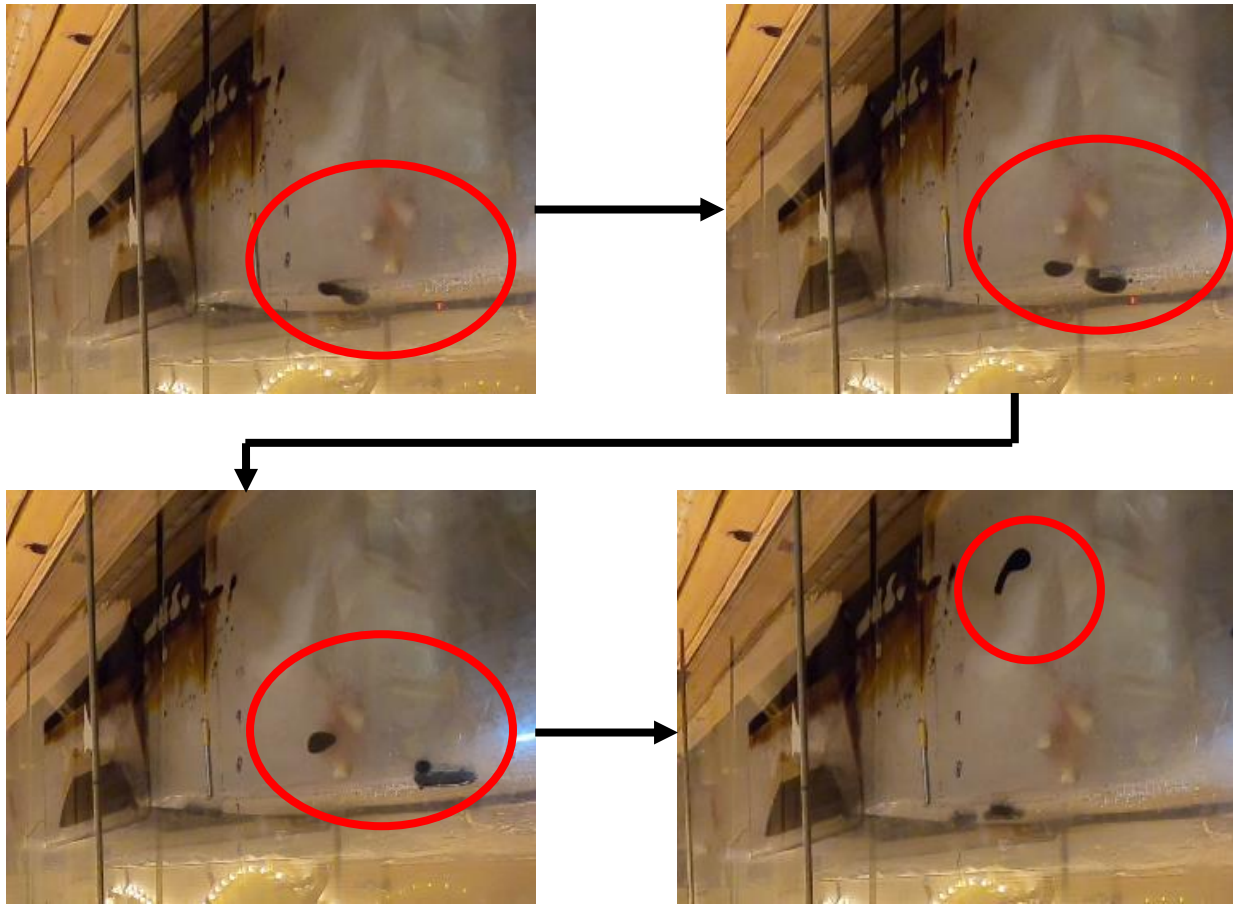
Figure 54: Ice melt evident due to oil interactions with fiberglass rebar structure. Oil droplets approach fiberglass rebar and are separated. One droplet continues downstream and the other is pushed laterally along the bottom side of the ice block and rises to the water surface along the side of the ice block.

Figure 55: Ice melt evident due to oil pooling along bottom of ice and flowing laterally in path
eroded in ice block.

For the third run, the water relative velocity was increased at smaller intervals to better
estimate the relative velocity where oil would be initially stripped from the cavity. For this run,
the water relative velocity was 0.09 +/- 0.05 m/s for 5 minutes, increased to 0.12 +/ 0.04 m/s for
5 minutes, and increased again to 0.14 +/- 0.03 m/s for 5 minutes. At these intervals, the oil
experienced ripple formation and slight edging blob formation was observed at 0.14 +/- 0.03 m/s.
Oil droplet formation occurred at 0.16 +/- 0.03 m/s (Figure 56). Relative velocity was held
constant at 0.16 +/- 0.03 m/s for about 4 minutes, until there was no longer droplet formation. It
was increased to 0.19 +/- 0.05 m/s, where droplet formation occurred frequently.
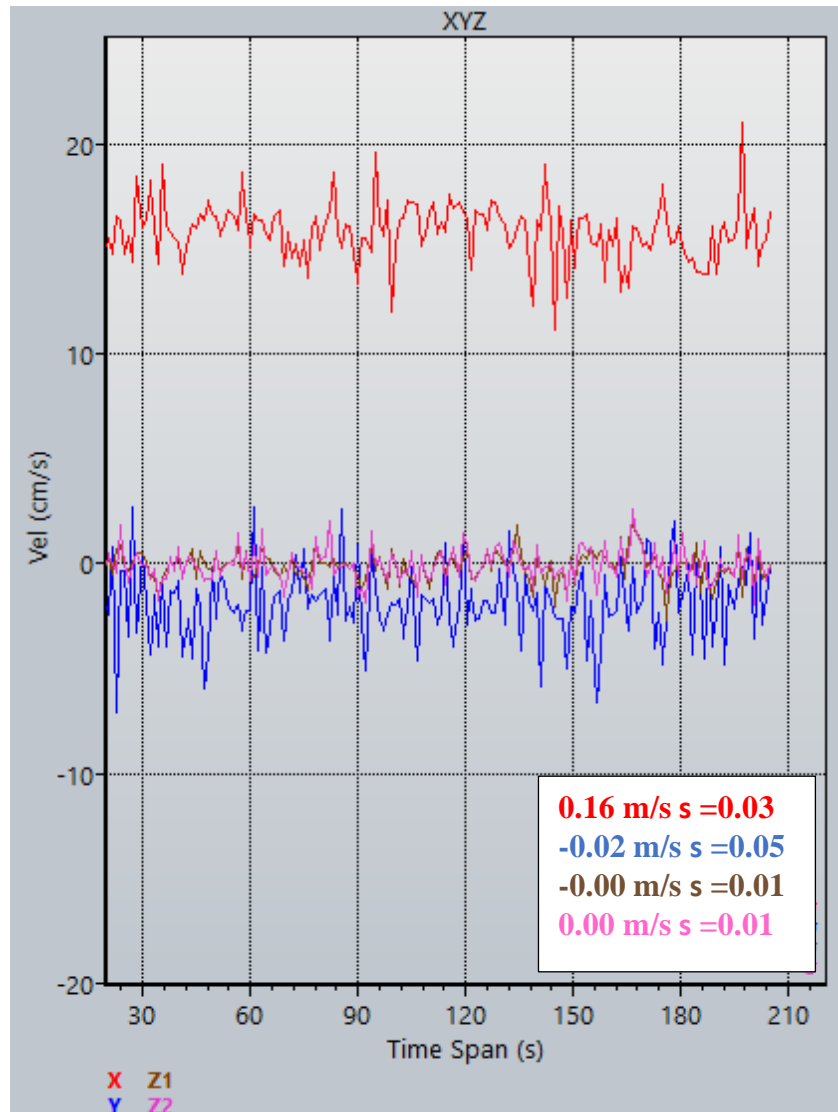
Figure 56: Run 3: relative velocity vs time when oil was stripped from cavity.

The amount of oil injected into the cavity varied slightly (Table 2), as different amounts of air were trapped under the ice each run (Figures 57-59). The injection ended when oil in the cavity was flush with the bottom of the ice. The volume of the cavity is about 3,900 mL, and the remaining space was occupied by trapped air.

Table 2: Volume of oil injected each run.

	Oil Injected (mL)
Run 1	3,054
Run 2	3,022
Run 3	1,983

Figure 57: Side view of oil and air in cavity (3,054 mL oil injected) (run 1).

Figure 58: Side view of oil and air in cavity (3,022 mL oil injected) (run 2).
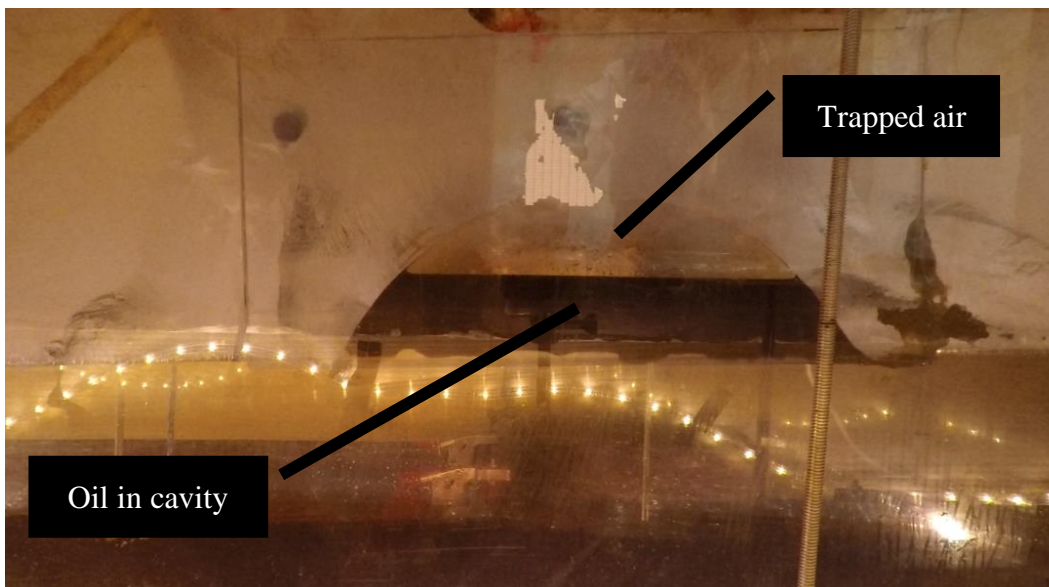
Figure 59: Side view of oil and air in cavity (1,983 mL oil injected) (run 3).

During the early runs, oil escaped from the alongside the polycarbonate and moved upward towards the water surface (Figure 60). Subsequent runs minimized this loss by adding

acrylic barriers that protrude an inch into the ice, perpendicular to the polycarbonate along its edges (Figure 17d).
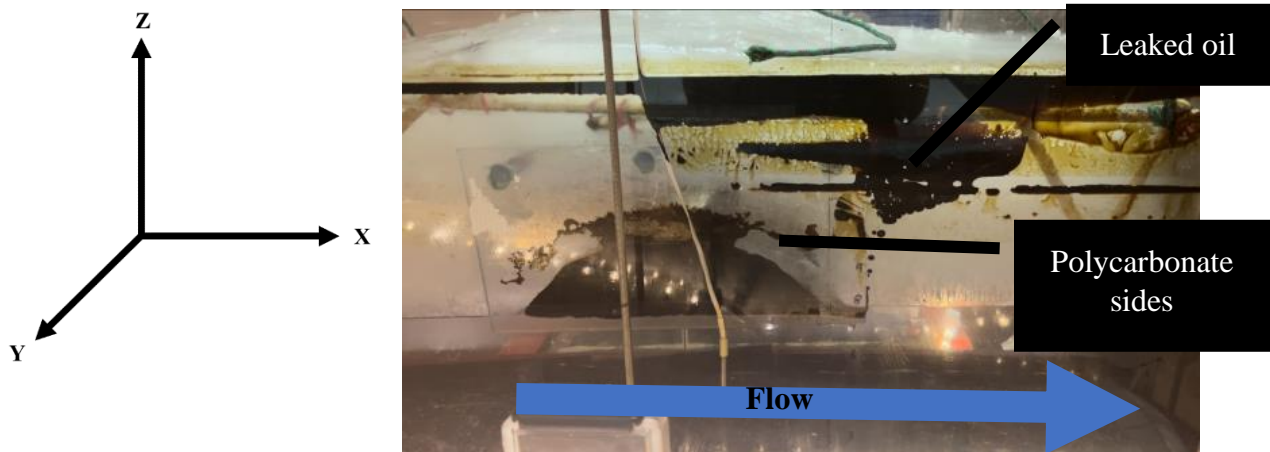
Figure 60: Oil leaked alongside polycarbonate towards water surface.

The water relative velocity for the fourth run started at 0.15 +/- 0.01 m/s, where ripple, edging blob, droplet, and pod formation were observed. The relative velocity was held constant for 5 minutes, until there was no longer droplet or pod formation. It was then increased to 0.17 +/- 0.01 m/s and more edging blobs occurred immediately (Figure 61). Oil droplet formation occurred frequently, and there was one pod formation during the 22-minute interval (Figure 62).
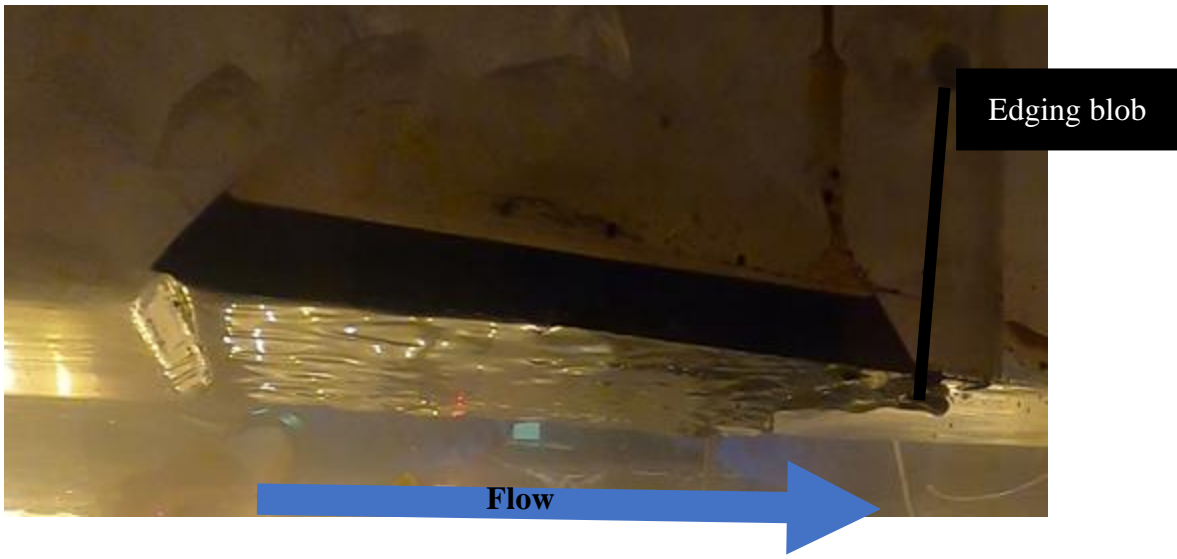
Figure 61: Edging blobs at 0.17 +/- 0.01 m/s (run 4).
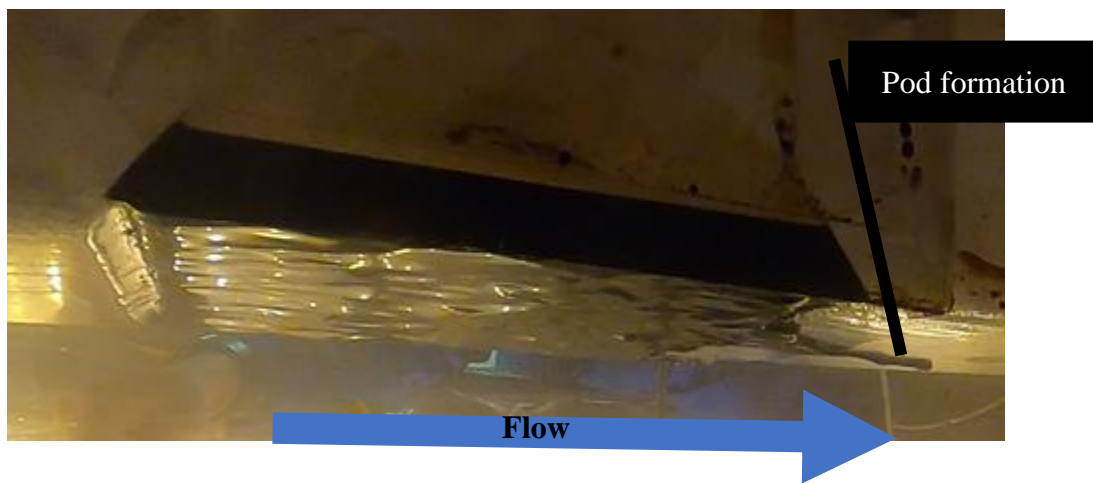
Figure 62: Pod formation at 0.17 +/- 0.01 m/s (run 4).

The propellors were turned off to stop the water relative velocity, a hole (1/4" diameter) was drilled through the ice to release air within the cavity, the hole was reclosed with shaved ice once the air was released, and more oil was injected into the cavity (Figure 63). This is not a typical process, but there was an opportunity to try a new method to release the trapped air, which is important to collect data with more consistency between trials.

Figure 63: Side view of oil and air in cavity (run 4).

The ice block had begun melting but maintained most of its shape. The water relative velocity was reset to 0.14 +/- 0.01 m/s. Ripple, edging blob, droplet, and pod formation all occurred immediately, but only ripple formation continued after 2 minutes (Figure 64). Droplets of oil remained stable on the underside of the ice block downstream of the cavity due to melted pockets and increased roughness in the ice block (Figure 65). After 5 minutes, the water relative velocity was increased to 0.15 +/- 0.01 m/s. Ripple formation continued and edging blobs and droplet formation were present. This was the last valid interval because the ice block had been in the flume for about an hour and melting had markedly deformed the cavity.
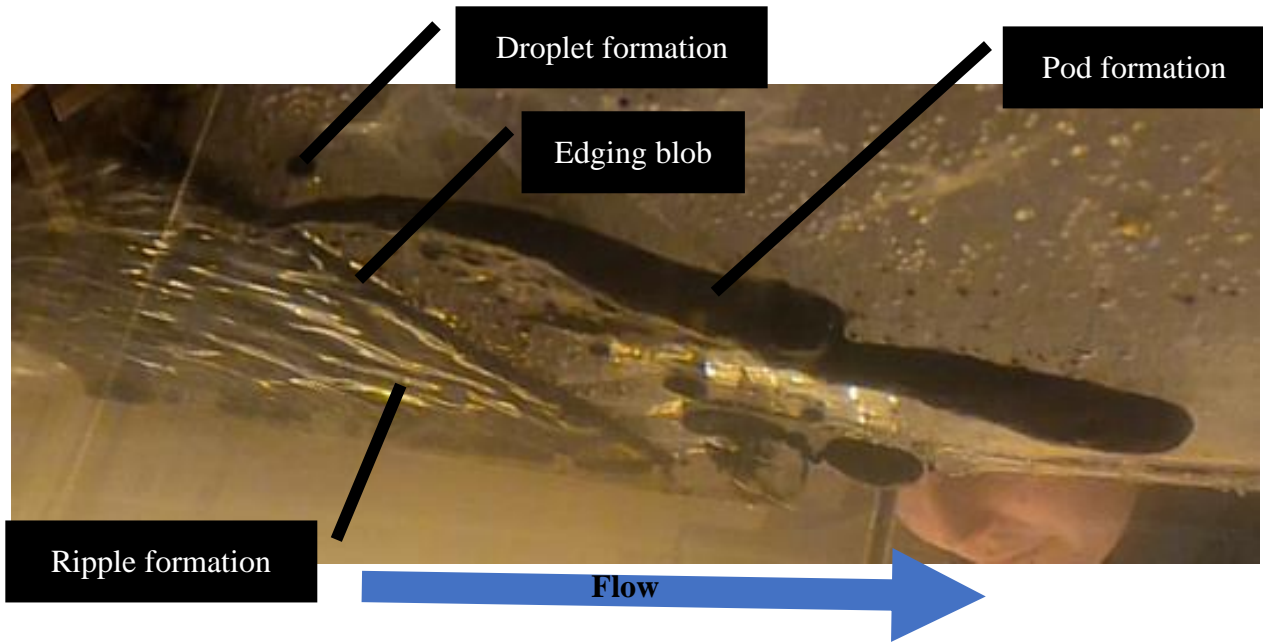
Figure 64: Oil formations at 0.14 +/- 0.01 m/s (run 4).

Figure 65: Stable oil droplets under ice (run 4).

After the trials were completed, Reynolds numbers were calculated for each relative velocity setting to characterize flow conditions as laminar or turbulent. Calculations determined each condition was laminar flow (Equation 2).

$$\text{Re} = \frac{U \times L \times \rho}{\mu}$$ (2)

Where,

Re = Reynolds number,

U = mean relative velocity (m/s),

L = distance from the middle of the cavity to the leading edge of the flat ice block

(1.37 m) (Figure 41),

ρ = water density at 4°C (998.97 kg/m^3),

and μ = water dynamic viscosity at 4°C (0.001569 kg/(m*s)).

Results for the initial runs are summarized in Tables 3-5.

Table 3: Initial trials summary (trials 1 and 2).

Trial		1	2
Oil Type		Fresh HOOPS	Fresh HOOPS
Volume of Oil Injected (mL)		3,054	3,022
Interval 1	Start - End Time (minutes from start of trial)	0-10	0-10
	Mean Relative Velocity (m/s)	0.11	0.10
	Oil Temperature (°C)	Not measured	-15
	Ice Surface Condition	Smooth	Smooth
	Reynolds Number	96062	87329
	Laminar or Turbulent?	Laminar	Laminar
	Ripples?	Yes	Yes
	Edging Blobs?	No	No
	Oil Droplets?	No	No
	Oil Pods?	No	No
Interval 2	Start - End Time (minutes from start of trial)	10-25	10-20
	Mean Relative Velocity (m/s)	0.22	0.20
	Oil Temperature (°C)	Not measured	Not measured
	Ice Surface Condition	Smooth	Smooth
	Reynolds Number	192123	174657
	Laminar, Transitional, Turbulent?	Laminar	Laminar
	Ripples?	Yes	Yes
	Edging Blobs?	Yes	Yes
	Oil Droplets?	Yes	Yes
	Oil Pods?	Yes	Yes

Table 4: Initial trials summary (trials 3 and 4, intervals 1-3).

Trial		3	4
Oil Type		Fresh HOOPS	Fresh HOOPS
Volume of Oil Injected (mL)		1,983	2,734
Interval 1	Start - End Time (minutes from start of trial)	0-5	0-5
	Mean Relative Velocity (m/s)	0.1	0.15
	Oil Temperature (°C)	Not measured	Not measured
	Ice Surface Condition	Smooth	Smooth
	Reynolds Number	78596	130993
	Laminar or Turbulent?	Laminar	Laminar
	Ripples?	Yes	Yes
	Edging Blobs?	No	Yes
	Oil Droplets?	No	Yes
	Oil Pods?	No	Yes
Interval 2	Start - End Time (minutes from start of trial)	5-10	5-27
	Mean Relative Velocity (m/s)	0.1	0.17
	Oil Temperature (°C)	Not measured	Not measured
	Ice Surface Condition	Smooth	Smooth
	Reynolds Number	104794	148459
	Laminar, Transitional, Turbulent?	Laminar	Laminar
	Ripples?	Yes	Yes
	Edging Blobs?	No	Yes
	Oil Droplets?	No	Yes
	Oil Pods?	No	Yes
Interval 3	Start - End Time (minutes from start of trial)	10-15	36-41
	Mean Relative Velocity (m/s)	0.14	0.14
	Oil Temperature (°C)	Not measured	Not measured
	Ice Surface Condition	Smooth	Smooth
	Reynolds Number	122260	122260
	Laminar, Transitional, Turbulent?	Laminar	Laminar
	Ripples?	Yes	Yes
	Edging Blobs?	Yes	Yes
	Oil Droplets?	No	Yes
	Oil Pods?	No	Yes

Table 5: Initial trials summary (trials 3 and 4, intervals 4-5).

Trial		3	4
Oil Type		Fresh HOOPS	Fresh HOOPS
Volume of Oil Injected (mL)		1,983	2,734
Interval 4	Start - End Time (minutes from start of trial)	15-19	41-44
	Mean Relative Velocity (m/s)	0.16	0.15
	Oil Temperature (°C)	Not measured	Not measured
	Ice Surface Condition	Smooth	Smooth
	Reynolds Number	139726	130993
	Laminar, Transitional, Turbulent?	Laminar	Laminar
	Ripples?	Yes	Yes
	Edging Blobs?	Yes	Yes
	Oil Droplets?	Yes	Yes
	Oil Pods?	No	No
Interval 5	Start - End Time (minutes from start of trial)	19-25	
	Mean Relative Velocity (m/s)	0.19	
	Oil Temperature (°C)	Not measured	
	Ice Surface Condition	Smooth	Significant ice melt
	Reynolds Number	165925	
	Laminar, Transitional, Turbulent?	Laminar	
	Ripples?	Yes	
	Edging Blobs?	Yes	
	Oil Droplets?	Yes	
	Oil Pods?	No	

The relative water velocities used in these trials are representative of currents under ice in the Arctic Ocean, which are typically under 0.25 m/s (Wadhams et al., 2006; Cole et al., 2017).

6. Conclusions

Due to an increase in shipping and development in the Arctic, the likelihood of oil spills is increasing and there is a need to improve trajectory modeling under sea ice. With the help of an advisory committee of sea ice and trajectory modeling experts, this thesis research successfully developed an experimental setup and protocol to collect data on the movement of oil under sea ice.

The MacFarlane Flume was modified to simulate Arctic conditions by achieving a water temperature of 4°C prior to the start of experiments. Insulation helped maintain that water temperature. At 4°C, the ice blocks maintained their shape for ~1 hour. Methods were developed to freeze ice blocks of specific dimensions and secure them in the flume. The size and shape of the cavity in the ice blocks (ellipse half cylinder across the span of the ice block width with a height radius of 3" and length radius of 4.5") was recommended by the advisory committee. The ice block creation process underwent several iterations until aluminum welded boxes were built to serve as molds. Initial experimental runs injected a known volume of oil, measured water relative velocity, and recorded the movement of oil.

Fresh HOOPS oil (-2°C, ~23cP) was stripped from the cavity at 0.16 m/s. As anticipated, the force pushing oil out of the ice cavity increased when the water relative velocity increased, which was observed by an increase in the amount of oil released.

Oil spill modelers have confirmed that the collected data will provide necessary information on the CSS of oil under ice to improve oil spill response models for the Arctic. Additional experimental runs will be completed to collect data and generate CSS estimates for several types of oil. Care must be taken to transition laboratory results into environmental predictions due to scaling (e.g., limited amount of oil released, limited ice area used,

permeability of sea ice vs. freshwater ice). Data characterizing the movement of oil under sea ice

is the first step to improve oil spill model projections in the Arctic, which is crucial to protect the

Arctic environment from the devastating impacts of future oil spills.

7. Future Work

This project should be continued and adapted for further data collection. Shear stress within the ice cavity will be calculated for *in-situ* conditions, including different relative velocities and various amounts of oil in the cavity. These calculations will be compared to water relative velocity (m/s) and observed erosions (number and type) over time to estimate CSS. Erosion volume and droplet size can be quantified using scale grids and software programs (e.g., Adobe Premiere Pro, Adobe Photoshop). CSS can be used by oil spill modelers during response to estimate mobilization and trajectory of oil under ice.

Different types of oil, weathering states, and volumes should be used. CSS is dependent on oil viscosity, water and ice velocity, and bed conditions (e.g., cavity shape, cavity size). Manipulating oil viscosity by an order of magnitude will produce a more robust algorithm that can be interpolated for other oils. Oil temperature measurements throughout the experimental run will capture changes in viscosity. Furthermore, combinations of oil and gas could be studied for potential releases involving both (e.g., well blowouts).

Additional cavity shapes and sizes will develop CSS estimates under different sea ice conditions. Increasing the number of cavities in series can prove whether oil will be contained by a downstream cavity, which is dependent on the distance between cavities and the relative velocity of the water.

Each trial should end when the ice blocks have been in the water for 20 minutes and only one relative velocity should be tested each trial due to ice melt. After 20 minutes, the cavity starts to experience significant melting that can impact ice roughness and hydraulic stresses on the oil. After the run is completed, the volume of oil remaining in the cavity should be measured. This can be calculated by measuring the depth of oil remaining in the cavity, and by pumping it

out using the injection tool with clean jars and tubing and setting the peristaltic pump in reverse. The volume can be calculated using the same method for the volume of oil injected, by dividing the mass of the oil by its density.

Ice blocks can be examined immediately after the completion of an experiment with a fine resolution to understand how the cavity changed throughout the experiment (Figure 66). These cavity measurements can be made using MeshLab (ISTI-CNS; Pisa, Italy), a 3D mesh processing software system. The underside of the ice block must be coated with sand to make it less transparent and then it is photographed. The shear stress / CSS estimates can be better if the initial and final dimensions of the cavity are known. To determine the initial cavity conditions, 3-4 ice blocks not used in experimental runs should be frozen, coated in sand, photographed, and processed in MeshLab. The known volume of the cavity should be compared to the volume determined by software analyses. Their time=0 cavity dimensions can be compared to those at the end of each run.
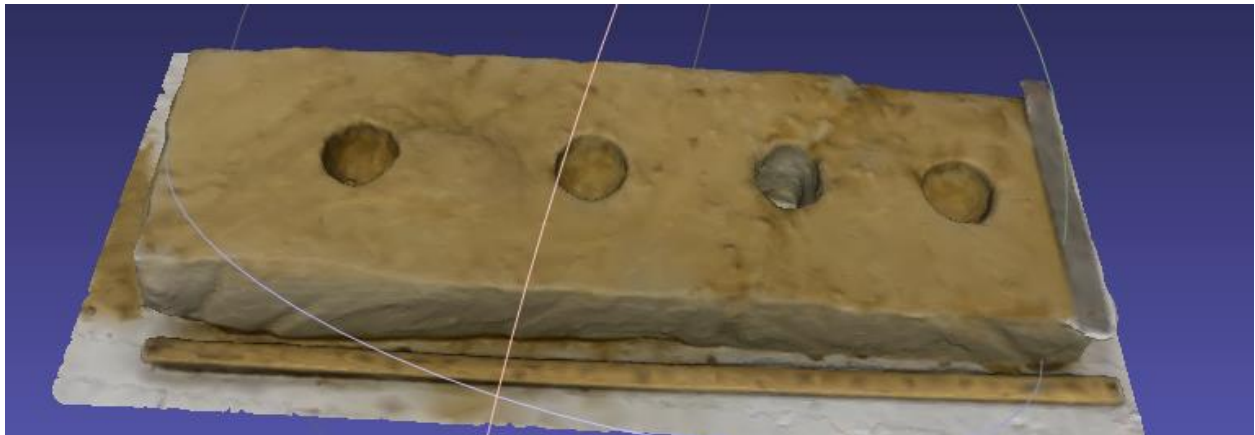
Figure 66: Model of ice cavities.

The velocimeter is located immediately downstream of the ice block, whereas the relative velocity of interest is within the ice cavity. The change in relative velocity is assessed to be insignificant between the ice cavity and where the probe is located, but this should be checked.

An upward looking velocimeter may be required for this future work but could not be located for this thesis research.

This project focused on the movement of oil under cavities in sea ice. While this is most likely the most dominant feature on the fate and behavior of oil, other features can impose considerable impacts, such as under ice permeability. Future work could use seawater ice to explore how saline induced permeability changes the oil and ice surface interactions and shear stresses.

Appendix A: Replicate Arctic Conditions SOP

1. Close flume access points and insulation sections. Place a weight on each of the three largest access points to hold them in place.

2. Fill flume to water depth of 7" in top section using well water. Secure hose in downstream turning section (Figure 67).

Figure 67: Location to secure hose in flume.

3. Place wooden support pieces in flume top section for stability in flume walls.

4. Turn on air conditioner.

5. Turn on flume motors to 2 Hz to circulate water for even cooling.

6. Prime pump and then turn on. To prime, open valve, enabling flow from garden hose to PVC pipe, and attach garden hose to PVC upstream of the pump and to the sink faucet. Turn on water until flume top section reaches 12" depth. Close valve, turn on pump, and then turn off water at faucet. Within a couple minutes there should be visible water flow from the PVC outlet pipe into the flume. If there is no flow from outlet pipe, repeat process while using a sump pump to remove water, keeping water at 12" depth.

7. Turn on the four chillers to their lowest set point.

8. Open outside doors and turn on fans as necessary to keep room as cool as possible.

9. Run system for about 12 hours, until flume water is at 4ºC.

Appendix B: Freeze Ice Blocks SOP

1. Weld two boxes out of ¼" aluminum. One box will have a flat bottom and the other will have a molded bottom for the ice cavity. The mold should be reinforced with extra aluminum, rather than hollow, to prevent collapsing from the force of water freezing. Welds should be smooth with a minimal radius.

2. Place welded box in freezer.

3. Add polycarbonate along the sides of the cavity.

4. Add fiberglass rebar structure with hook. Measure hook placement to the center of welded box. Suspend rebar ~1" from bottom of welded box using rope tied to the fiberglass rebar and clamped to sides of the box. Fill welded box with cold water until a quarter of the hook is submerged. Tie hook in place to ensure it remains upright.

5. Add C-shaped wooden supports to welded box to support welds and prevent box from bowing outward (Figure 15).

6. Close freezer and keep closed until ice blocks are frozen. Time to freeze depends on freezer contents.

7. Remove ice block from box once it is frozen. Line warm water tank with plastic and fill with warm tap water until water reaches 5" depth. Align freezer to position center of ice block under hoist. Ensure support posts are vertically level on each end of the hoist sliding support beam. Use hoist controls to hook ice block to hoist and place ice block into warm water tank by raising ice block with welded box, sliding hoist along its beam, and lowering ice block into warm water tank. To slide hoist, push its metal casing with a pole. Let the box sit in the warm water for a minute, then slowly lift ice block with the hoist while holding the metal box down. If ice block does not release from welded box,

then return briefly to warm water tank, but ensure minimal melting around edges of ice block. Return ice block to freezer using hoist and store until needed.

8. Drill hole (¼" diameter) into ice block with cavity through its top and into the cavity. This will allow trapped air in the cavity to escape once the ice block is in the flume.

Appendix C: Experimental Protocol SOP

1. Prepare approximately 4 L of oil (enough to fill ice cavity). Record mass of empty jar with its lid and fill with HOOPS. Record mass of jar with its lid and filled with oil. Cool oil in freezer to about -2℃ to minimize bottom ice melt.

2. Secure temperature data logger in designated location, near location of ice cavity. Start to record temperature of water near oil throughout experiment.

3. Ensure support posts are vertically level on each end of the hoist sliding support beam.

4. Prepare Vectrino for installation: attach Vectrino to its stand (slide Vectrino probe through hose clamps and tighten hose clamps around the body in their designated locations), wipe probe with a Kimwipe, plug cable into computer and Vectrino, and prepare the program for data collection.

   a. Vectrino software steps:

      i. Open Vectrino Profiler program.

      ii. Select Communication tab, Connect, and Vectrino Profiler.

         1. Change port speed to 937,500 and port timeout to 2,000 ms.

         2. Select Apply.

      iii. Select Configuration icon. ⊞

         1. Under File Parameters tab, set location for files to be saved in, and select Apply.

         2. Under Doppler tab, ensure:

            a. Sampling rate = 25 Hz,

            b. Ping algorithm = adaptive,

            c. Adaptive check = once,

        d. Velocity range = 1.5,

        e. Range to first cell = 40,

        f. Range to last cell = 68,

        g. Select Apply.

    3. Under Bottom Check tab, ensure:

        a. Enable box is checked,

        b. Maximum depth = 254 mm,

        c. Minimum depth = 152 mm,

        d. Select Apply and OK.

  iv. Select Save icon.

    1. This icon must be highlighted to save data to the specified location when the program is started and stopped.

5. Prepare tubing used for injecting oil. Cut length of tubing to reach from ice cavity positioned in flume, through peristaltic pump, and into oil jars. Record mass of tubing that will be used during injection process.

6. Tape injection tubing to apparatus that navigates tubing into ice cavity. Place other end of tubing into peristaltic pump and secure, leaving enough tubing to reach bottom of oil jar.

7. Align freezer to position center of downstream ice block under hoist.

8. Place three GoPros in designated locations. The GoPros will record a side view of oil in the cavity, an angled view pointed at the cavity and underside of the ice, and an angled upward view that is focused on oil in the cavity. Connect GoPros to application. This cannot be completed sooner because the batteries die quickly under cold temperatures.

  a. GoPro settings

      i. GoPro Hero 8 Black (1)

         1. SD Card: 256 GB

         2. Quality: 1440 p / 60 fps

         3. Location: 3-dimensional view including downstream end of ice cavity and underside of ice

      ii. GoPro Hero 8 Black (2)

         1. SD Card: 128 GB

         2. Quality: 1440 p / 60 fps

         3. Location: Suction cup set up on right motor side to view oil in cavity at water interface

      iii. GoPro Hero 4

         1. SD Card: 32 GB

         2. Quality: 1080 p / 30 fps

         3. Location: Side view of cavity on left motor side

9. Adjust flume motor settings to speed that experimental run will start at and press "Stop."

10. Turn off pump connected to plumbing for chillers.

11. Turn off all chillers.

12. Remove inlet and outlet pipes at union connections closest to the flume and pull out of insulation.

13. Remove insulation over section where ice blocks will be secured.

14. Add 20 g of kaolinite clay to flume water to improve Vectrino readings. Stir water vigorously with metal rod to prevent clay from settling.

15. Secure injection apparatus in flume using clamps and the wooden flume wall supports.

16. Hoist downstream ice block (ice block with cavity) into flume by attaching hoist cable to hook frozen in ice block, raising the cable, sliding hoist over the flume using pole, and lowering ice block while guiding it into flume.

17. Detach hoist hook from ice block and return hoist over freezer by sliding it on beam.

18. Secure ice block in flume (with its downstream end 12.5 ft from upstream end of the flume top section, as marked in flume) by tying ropes into the ice to the bolts threaded in along top of flume. Level bottom of ice block in flume.

19. Align freezer with center of upstream ice block under hoist.

20. Repeat steps 16-18 with upstream ice block (flat bottom), placing it upstream of the ice block with a cavity.

21. If there is air trapped in the cavity, redrill hole through ice block to allow trapped air to escape. Refill and pack hole with ice shavings from freezer.

22. Begin recording on all three GoPros.

23. Take oil temperature and inject oil into ice cavity using peristaltic pump apparatus. Keep tubing submerged in oil jars to avoid injecting air into the cavity. Slide apparatus down in cavity as it fills with oil to prevent tubing from touching oil. Turn off pump when cavity appears full of oil, indicated by oil leveled with bottom of ice block.

24. Remove injection apparatus.

25. Secure Vectrino in place with its red piece facing downstream and begin data collection by selecting the start icon.   ▶

    a. Select Profiles SNR tab and record signal to noise ratio (SNR). This value should be greater than 10, with higher values indicating better results.

    b. Select BottomCheck Bottom Distance tab and record bottom check distance.

    c. Select Profiles Correlation and record correlation value. This should be at least 70%, and preferably as close as possible to 100%.

    d. If any of these measurements are out of range, then the data could be compromised. Troubleshoot potential interferences (e.g., add more clay, wipe probe with Kimwipes to remove particles and bubbles, level stand, remove obstructions causing turbulence, center probe across flume width).

26. Replace top insulation.

27. Turn on motors, flash string lights in flume to mark start time on GoPro footage, and record start time.

28. Increase relative velocity until oil mobilizes from the cavity. Hold relative velocity constant while oil is mobilizing until there is no more oil movement. Flash string light in flume to document the increase in relative velocity in the GoPro footage. Stop and restart Vectrino data collection each change in relative velocity to save each setting as a different file. Record time of each change in relative velocity.

29. Check GoPros periodically for their red recording light, and replace batteries as needed, around an hour of recording.

30. Run experiment until all oil is excavated from the cavity or when there has been significant ice melt (~20 minutes). Then stop data collection on Vectrino Profiler and turn off flume motors.

31. Select Data tab in Vectrino Profiler and export all files as MatLab files, and then disconnect Vectrino.

32. Run MatLab files through MatLab code to collect graphed data.

    a. Open MatLab.

b. Home, Open, select FilteringData.m

c. Load file

    i. Home, Set Path, Add Folder, select folder that contains file, Save, Close

    ii. Double click file in directory panel on lefthand side.

    iii. Load command will populate in command window.

```
Command Window
  >> load('C:\Users\jml416\OneDrive - USNH\CRRC\Oil Under Ice\Data\12_14\VectrinoData11152022.348.22.Vectrino Profiler.00000.m
fx >> |
```

d. Copy and paste file name into Line 4, replacing current file name in the code.

e. Editor tab, select run.

f. Mean relative velocities are located under Figure 2 "X-Velocity Data: Raw, Cleaned and Filtered." Select Tools and Data Statistics to record mean relative velocities for each file.

33. Files can also be replayed through Vectrino Profiler:

a. Open Vectrino Profiler.

b. Data, Data File Playback, Browse, select file, Apply, OK.

c. Select Time Series Options icon,

    i. Adjust to length of time of trial in seconds.

d. Select Play icon to replay data.

34. Record mass of residual oil in tubing and jars. Tare a container to hold tubing with residual oil. Record mass of tubing with residual oil, zero balance, and record mass of each jar with residual oil.

35. Calculate volume of oil injected into the cavity.

a. Use hydrometer with specific gravity (range of 0.85 – 0.90 for fresh HOOPS) to determine density of oil at -2°C.

    b.   Subtract mass of residual oil in jar from mass of jar full of oil. If more than one jar was used, then total to find mass of oil injected.

    c.   Subtract the mass of residual oil in tubing from total mass of oil injected.

    d.   Divide final mass of oil injected by the density of oil to find volume of oil injected.

36. Upload GoPro footage from SD cards onto a hard drive, organized in folders by date and location of camera. Clear SD cards and charge GoPro batteries.

37. Upload temperature data to hard drive, organized in folders by date.

38. Drain flume, open access points, and clean oil from flume, Vectrino, and all materials used.

Appendix D: Raw Data: Mass of Oil Injected

The table below displays the data of mass of oil injected in each run performed. For each run, the mass of each container and its lid were taken when it was filled with oil, and again after oil was injected from the container. The difference in these values provide the mass of oil injected from each container. The mass of the tubing was also taken before and after oil was injected. The difference in these values provided the mass of oil that was removed from the containers but did not get into the ice cavity. Therefore, this value was subtracted from the mass of oil injected from the containers to obtain the value of oil injected into the ice cavity.

Mass (g)

Run	Tubing		Oil Container 1 (with lid)		Oil Container 2 (with lid)		Oil Container 3 (with lid)		Oil Delivered to Ice Cavity
	No oil	Residual oil	Oil filled	Residual oil	Oil filled	Residual oil	Oil filled	Residual oil	
1	155.3	189.9	1584.1	697.3	1645.6	701.7	1596.0	701.6	2690.5
2	156.0	177.7	1591.2	739.5	1637.4	722.7	1658.0	740.2	2662.5
3	239.2	229.4	1616.1	702.8	1446.3	622.6	N/A	N/A	1746.8
4	222.0	268.3	1608.3	1029.9	1631.5	697.7	1645.9	700.0	2411.8

List of References

Ahlenius, H. 2023. Population Distribution in the Circumpolar Arctic, by Country (Including
Indigenous Population). UNEP/GRID-Arendal. Available online:
https://www.grida.no/resources/7154 (accessed on January 13, 2023).

Cole, S., Toole, J., Lele, R., Timmermans, M.-L., Gallaher, S., Stanton, T., Shaw, W., Hwang,
B., Maksym, T., Wilkinson, J., Ortiz, M., Graber, H., Rainville, L., Petty, A., Farrell, S.,
Richter-Menge, J., and Haas, C. 2017. Ice and ocean velocity in the Arctic marginal ice
zone: Ice roughness and momentum transfer. University of California Press.
https://doi.org/10.1525/elementa.241.

Comiso, J. 2012. Large Decadal Decline of the Arctic Multiyear Ice Cover. Journal of Climate
25 (4): 1176–93. https://doi.org/10.1175/JCLI-D-11-00113.1.

Daling, P.S., Brandvik, P.J., Mackay, D., and Johansen, O. 1990. Characterization of crude oils
for environmental purposes. Pp. 119-138 in Proceedings of the 13th Arctic and Marine
Oil Spill Program (AMOP) Technical Seminar. Environment Canada, Ottawa, Ontario.

Environment and Climate Change Canada (ECCC). 2016. Chapter 1: Interpreting Ice Charts.
Available online: https://www.canada.ca/en/environment-climate-change/services/ice-
forecasts-observations/publications/interpreting-charts/chapter-1.html (accessed on
January 13, 2023).

Forsman, N. and Forsman, B. 2019. Oil spill risk assessment methodology for extreme
conditions, including Arctic. GRACE, Ref. 2870036.

Glaeser, J., and Vance, G. 1972. A Study of the Behavior of Oil Spills in the Arctic. Offshore
Technology Conference. https://doi.org/10.4043/1551-ms.

Gloekler, M. 2021. Development of a Sunken Oil Transport Tool using Mesoscale Experiments.

    University of New Hampshire, Doctoral Dissertation. Available online:

    https://scholars.unh.edu/dissertation/2571/ (accessed on January 13, 2023).

Manning, J., Verfaillie, V., Barker, C., Berg, C., MacFadyen, A., Donnellan, M., Everett, M.,

    Graham, C., Roe, J., and Kinner, N. "Responder Needs Addressed by Arctic

    Maritime Oil Spill Modeling." 2021. Journal of Marine Science and Engineering 9, no. 2:

    201. https://doi.org/10.3390/jmse9020201.

Markus, T., Stroeve, J. C., and Miller, J. 2009. Recent changes in Arctic sea ice melt onset,

    freeze up, and melt season length, J. Geophys. Res., 114, C12024,

    https://doi.org/10.1029/2009JC005436.

NASA. 2022. Arctic Sea Ice Minimum Extent | NASA Global Climate Change. Vital Signs of

    the Planet. Available online: https://climate.nasa.gov/vital-signs/arctic-sea-ice (accessed

    on January 13, 2023).

National Academies of Sciences, Engineering, and Medicine. 2014. Responding to Oil

    Spills in the U.S. Arctic Marine Environment. Washington, DC: The National Academies

    Press. https://doi.org/10.17226/18625.

National Pollution Funds Center. 2006. Oil Spill Liability Trust Fund (OSLTF), Annual Report

    FY 2002 – FY 2006. Available online: www.uscg.mil/npfc (accessed on January 13,

    2023).

Nielsen, D.M., Pieper, P., Barkhordarian, A., Overduin, P., Ilyina, T., Brovkin, V., Baehr, J., and

    Dobrynin, M. 2022. Increase in Arctic coastal erosion and its sensitivity to warming in

    the twenty-first century. National Climate Change. 12, 263–270.

    https://doi.org/10.1038/s41558-022-01281-0.

Nortek AS. 2018. Comprehensive Manual. Available online:

    https://www.nortekgroup.com/assets/software/N3015-030-Comprehensive-Manual-

    Velocimeters_1118.pdf (accessed on January 13, 2023).

Notz, D., and Bitz, C. 2017. Sea ice in Earth system models. Pp. 304-325 in Sea Ice (Third

    Edition). John Wiley & Sons, Chichester, UK, Hoboken, NJ.

Perovich, D., Meier, W., Tschudi, M., Hendricks, S., Petty, A. A., Divine, D., Farrell, S.,

    Gerland, S., Haas, C., Kaleschke, L., Pavlova, O., Ricker, R., Tian-Kunze, X., Webster,

    M., and Wood, K. 2020. "Arctic Report Card 2020: Sea Ice."

    https://doi.org/10.25923/N170-9H57.

Persson, O., and Vihma, T. 2017. The atmosphere over sea ice. Pp. 160-196 in Sea Ice (Third

    Edition). John Wiley & Sons, Chichester, UK, Hoboken, NJ.

Rodrigue, J-P. 2017. Polar Shipping Routes. The Geography of Transport Systems. New York,

    USA: Dept. of Global Studies & Geography, Hofstra University.

    https://transportgeography.org/contents/chapter1/transportation-and-space/polar-

    shipping-routes/ (accessed on January 13, 2023).

Thompson, K. 2016. What Happens in the Arctic Doesn't Stay in the Arctic. Greenpeace

    Research Laboratories Technical Report (Review) No. 04-2016. Available online:

    http://archivo-es.greenpeace.org/espana/Global/espana/2016/report/artico/ArticoEN-

    LR.pdf (accessed on January 13, 2023).

Wadhams, P., Wilkinson, J., and McPhail, S. 2006. A new view of the underside of Arctic sea

    ice. Geophysical Research Letters, Vol. 33: L04501.

    https://doi.org/10.1029/2005GL025131.

Wilkinson, J., Beegle-Krause, C., Evers, KU., Hughes, N., Lewis, A., Reed, M., and Wadhams, P. 2017. Oil spill response capabilities and technologies for ice-covered Arctic marine waters: A review of recent developments and established practices. Ambio 46 (Suppl 3), 423–441. https://doi.org/10.1007/s13280-017-0958-y.

Wilkinson, J., Wadhams, P., and Hughes, N. 2007. Modelling the Spread of Oil under Fast Sea Ice Using Three-Dimensional Multibeam Sonar Data. Geophysical Research Letters 34 (22): L22506. https://doi.org/10.1029/2007GL031754.

Zelenke, B., O'Connor, C., and Barker, C. 2012. "General NOAA Operational Modeling Environment (GNOME) Technical Documentation." Available online: https://response.restoration.noaa.gov/sites/default/files/GNOME_Tech_Doc.pdf (accessed on January 13, 2023).